MEASURED DIRECTIONAL REFLECTANCES OF CHARS IN THE UV, VISIBLE, AND NEAR INFRARED

report to
JET PROPULSION LABORATORY

Contract No. 950867

Subcontract Under NAS7–100

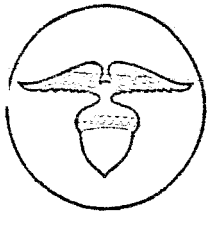

Arthur D. Little, Inc.

MEASURED DIRECTIONAL REFLECTANCES OF CHARS IN THE UV, VISIBLE, AND NEAR INFRARED

Report to

JET PROPULSION LABORATORY

Contract No. 950867

Subcontract under NAS7-100

March 1966

C-66658

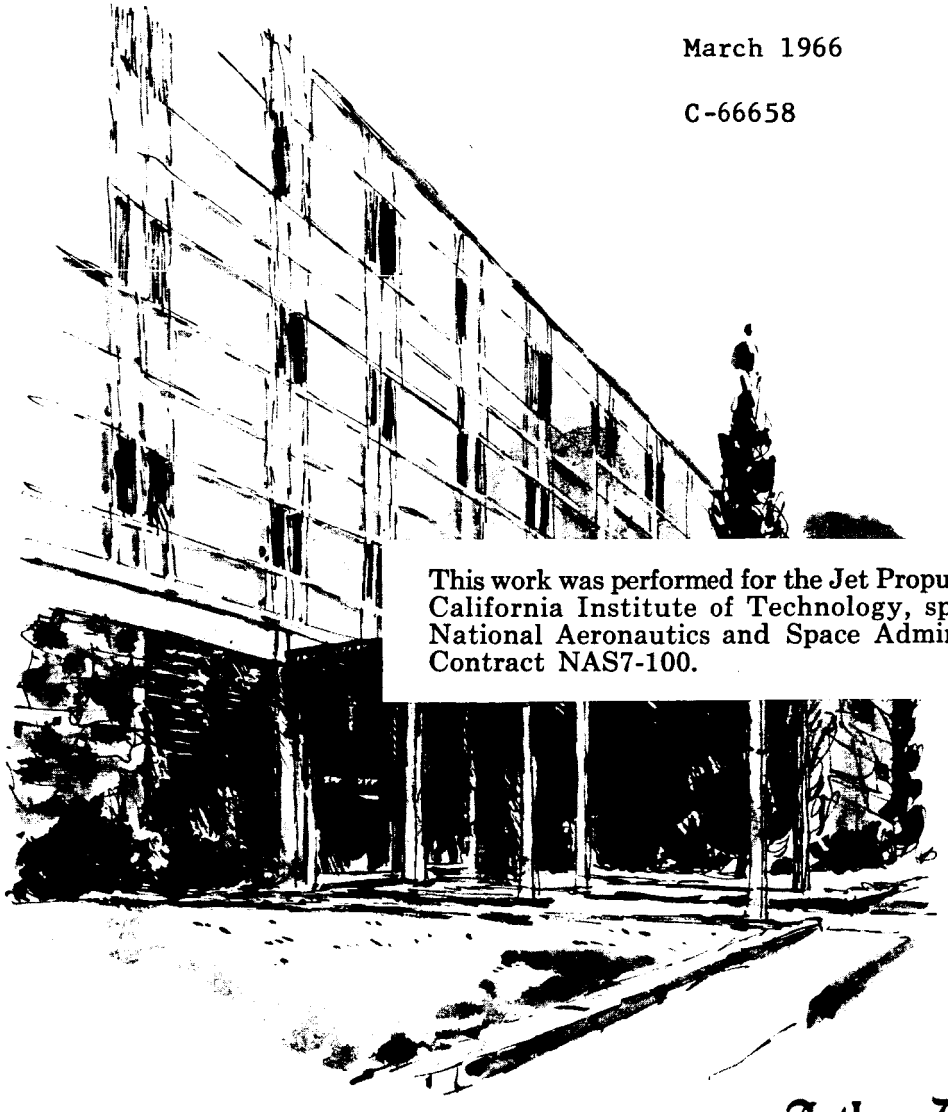

This work was performed for the Jet Propulsion Laboratory, California Institute of Technology, sponsored by the National Aeronautics and Space Administration under Contract NAS7-100.

Arthur D. Little, Inc.

TABLE OF CONTENTS

LIST OF TABLES

LIST OF FIGURES

I. INTRODUCTION

This report summarizes the results of a program conducted at Arthur D. Little, Inc., and sponsored by the Jet Propulsion Laboratory to develop a technique for measuring the reflectances of carbonaceous chars at room temperature and at elevated temperatures. The ultimate objective is to develop a way of predicting the behavior of such materials, particularly their radiant heat absorption and reradiation, in the atmospheric entry situation. In this program the problem was reduced to consideration of reflectances of precharred samples in a quiescent argon atmosphere.

Measurements were made at four wavelengths--0.2, 0.4, 0.65, and 1.0 micron--and at two temperatures--room temperature and 2200°F, the highest temperature at which we were able to make satisfactory measurements.

At entry an ablator receives a significant amount of gas-cap radiation at near-glancing angles. Therefore, the directional reflectance of these materials is of great interest, particularly at these near-glancing angles; and the apparatus is designed to test for angular sensitivity. Measurements were made at four (incident) angles: as near normal as our apparatus would allow (33° from the pole), as near glancing as our apparatus would allow (72° from the pole), and at two intermediate angles (45° and 60°).

Reflectances are measured by a three-dimensional goniometric technique. Both the source and the detector can be rotated independently in spherical coordinates about a sample at the origin. Sequential readings are taken by stepping through a number of fixed angles around the sample, and reflectance is determined from the sum of the sequence of readings. Both the incident and reflected radiation are measured in the same way, so that the method is absolute and requires no reflectance standard.

An advantage of the method is that the errors are well known and can be readily estimated. A disadvantage is that a hot reflectance determination takes over an hour, during which time the condition (and reflectance) of a sample may change.

Section II of this report describes the Method, Section III the Results. Further details and equations are given in the Appendices.

II. METHOD

A. PRINCIPLE OF MEASUREMENT

The quantity measured is directional spectral reflectance ($R_{\psi\lambda}$) the ratio of radiation at one wavelength reflected from a flat sample into a surrounding hemisphere to radiation at the same wavelength incident onto the sample in a narrow beam. This reflectance ($R_{\psi\lambda}$) may be used rigorously to determine corresponding values of directional spectral absorptance and directional spectral emittance.

$R_{\psi\lambda}$ was measured by sequential collection of reflected radiation; in this technique a detector is moved through a succession of locations over the hemisphere surrounding the sample (Figure 1) and the readings are summed. The strength of the incident radiation beam is measured by aiming the source beam directly into the detector. Reflectance is calculated as the ratio of the sum of the reflected readings to the single incident reading. The sample may be at room temperature or may be heated while its reflectance is being measured. The method is absolute and requires no standard reflectance. Further discussion is included in Appendix B ("Method of Measurement") and Appendix D ("Calculation of Reflectance").

B. APPARATUS

For simplicity of illustration, Figure 1 shows the sample and hemispherical coordinate system around it fixed, while the detector is made to move over the coordinate hemisphere. In an actual apparatus, it is more practical to do the reverse--i.e., to fix the position of the detector (with respect to the laboratory bench) and to rotate the sample, incident beam, and coordinate system. The result is unchanged, though the angular relationships are not quite as easy to visualize by looking at the apparatus.

A schematic diagram of the optical system is shown in Figure 2. The equipment was designed so that the source could be locked at a fixed incident angle, ψ , with respect to the sample and the combination of source and sample rotated with the sample at the origin. The source and collection optics were located at a radius of approximately 10 inches.

Incident radiation was focused into a spot smaller than the 1/2-inch diameter sample, and the beam was centered on the sample so that negligible radiation was lost or reflected off other material such as the sample holder. Virtually all of the incident radiation fell on the sample. Within this constraint, the incident image was broadened by defocusing as much as possible to obtain statistical smoothing with regard to sample pore structure.

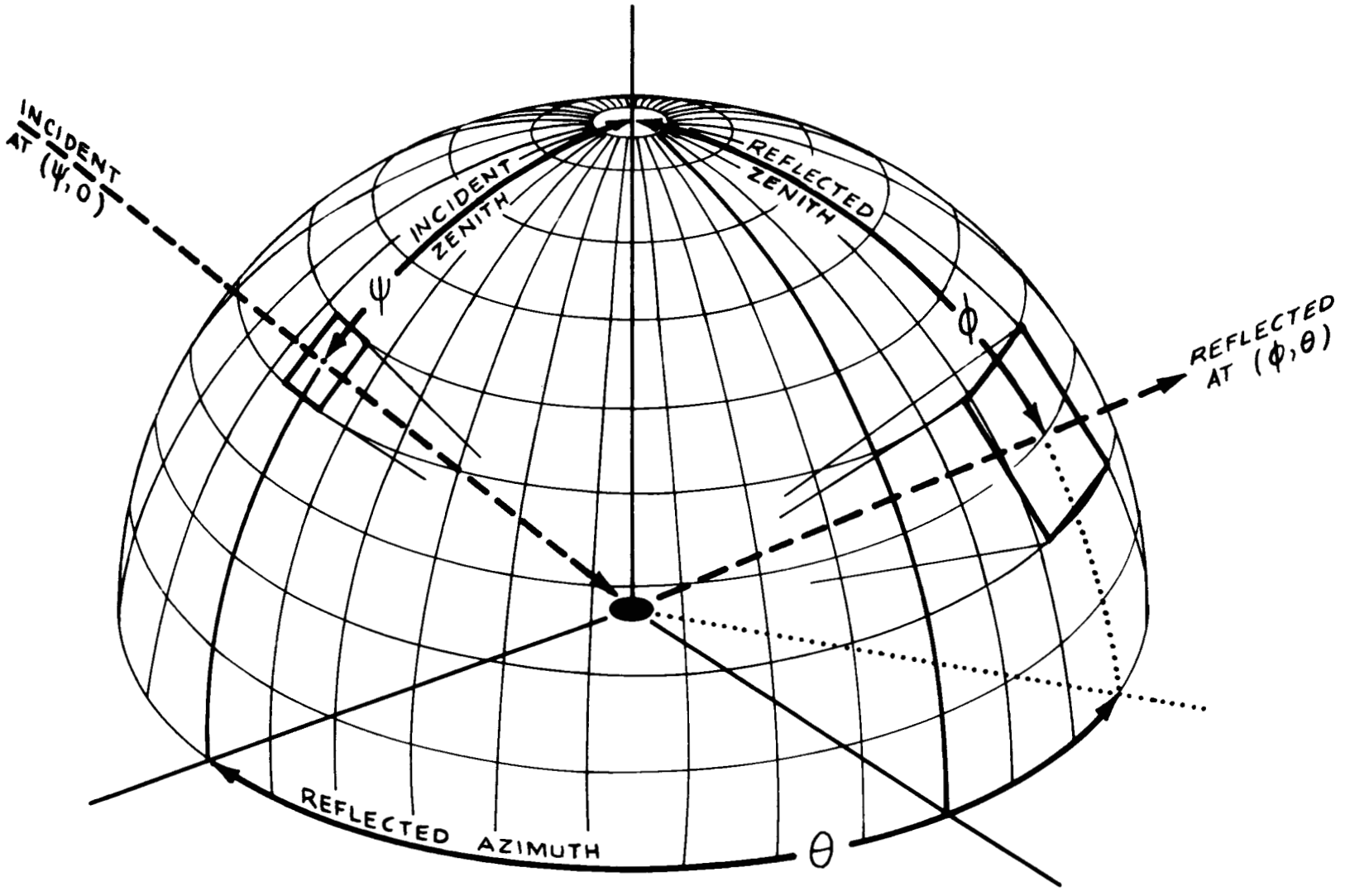

FIGURE 1 - REFLECTANCE COORDINATE SYSTEM

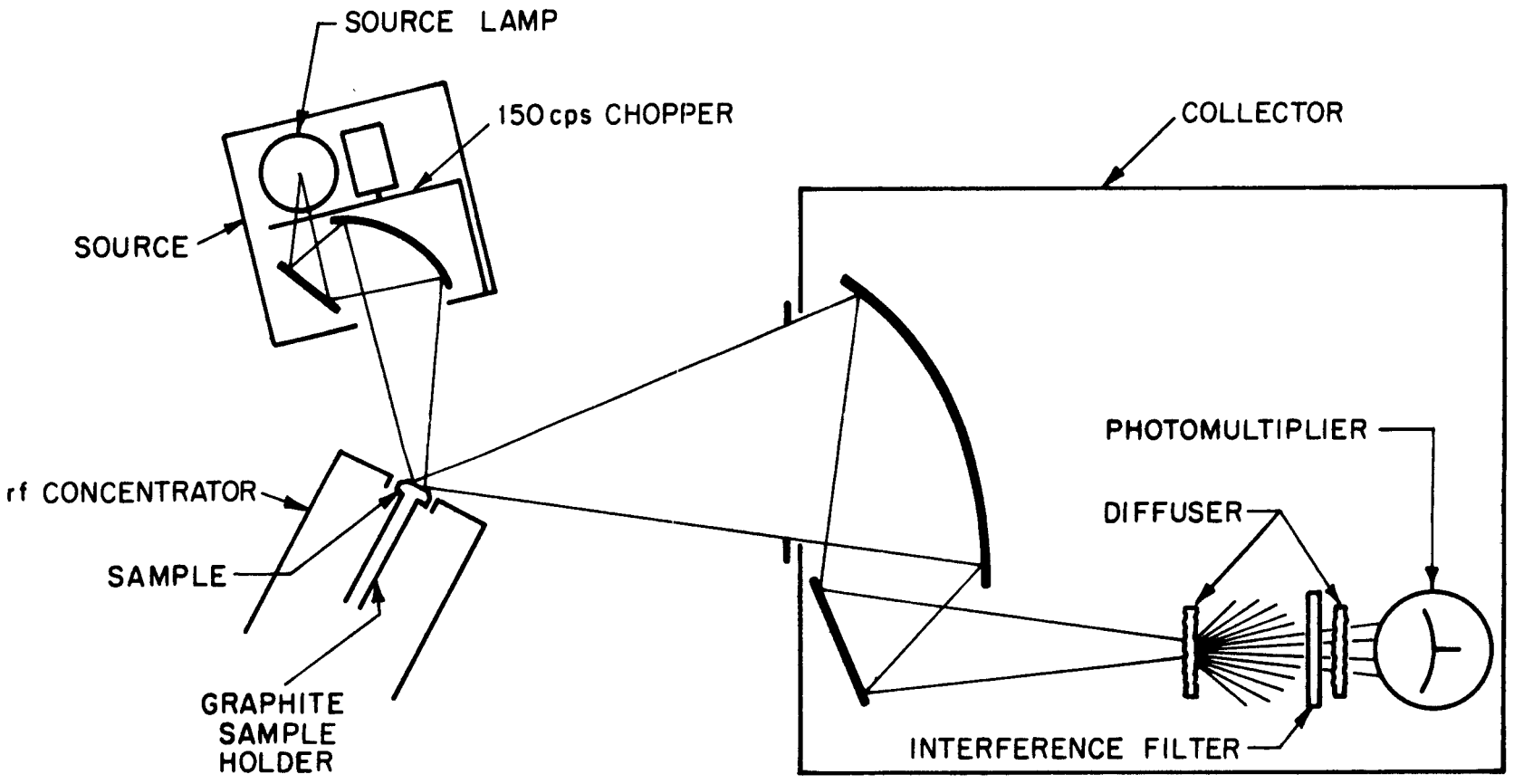

FIGURE 2 - OPTICAL SCHEMATIC

Radiation reflected from the sample was collected through a large, square aperture followed by a front-surfaced optical and diffuser system, which was designed to collect all of the radiation coming through the aperture with a minimum of spurious angular or spatial sensitivity. The radiation then passed through a single-band interference filter to a photomultiplier.

A functional block diagram of the equipment is shown in Figure 3. The reflectance measuring system uses chopped radiation to provide discrimination against self-radiant emission by the sample when it is hot. The incident beam was chopped at 150 cycles per second and the chopped radiation detected by a photomultiplier with amplifiers arranged to discriminate against all but the chopping frequency.

Since the samples were heated by radio-frequency induction, they had to be electrically conductive. Not all of our original samples were conductive, even though charred; some had to be made conductive by heating for one hour at 2500°C, a process carried out at JPL.

The sample can be surrounded by argon at one atmosphere by enclosing it in a mylar bag, which is then filled with the gas and collapsed a number of times to remove contaminants with a minimum of gas wastage. The sample can be handled and adjustments made through gloves in the bag.

Figure 4 shows three views of the actual apparatus.

C. MEASUREMENT PROCEDURE

The optical absorption of air was found to be indistinguishable from the absorption by argon at 0.4, 0.65, and 1.0 micron. However, air did absorb at 0.2 micron (ozone is generated). At this wavelength even a moderately pure argon atmosphere was sufficient to reduce UV absorption to a negligible level.

Cold samples at blue, red, and IR were usually measured in air, cold samples at UV in moderate purity argon, and hot samples at all wavelengths in the highest purity argon.

To provide an argon atmosphere, the mylar bag was collapsed and filled two complete cycles for cold UV measurements and four complete cycles for hot sample measurements.

First the sample was mounted. Then it was swung away, the incident beam was aimed into the collecting aperture, and a reading was taken. The sample was swung back in position and locked, and 22 separate reflected readings were taken, each at a different angular position on the coordinate hemisphere. The last step was a second incident reading at the end of the run.

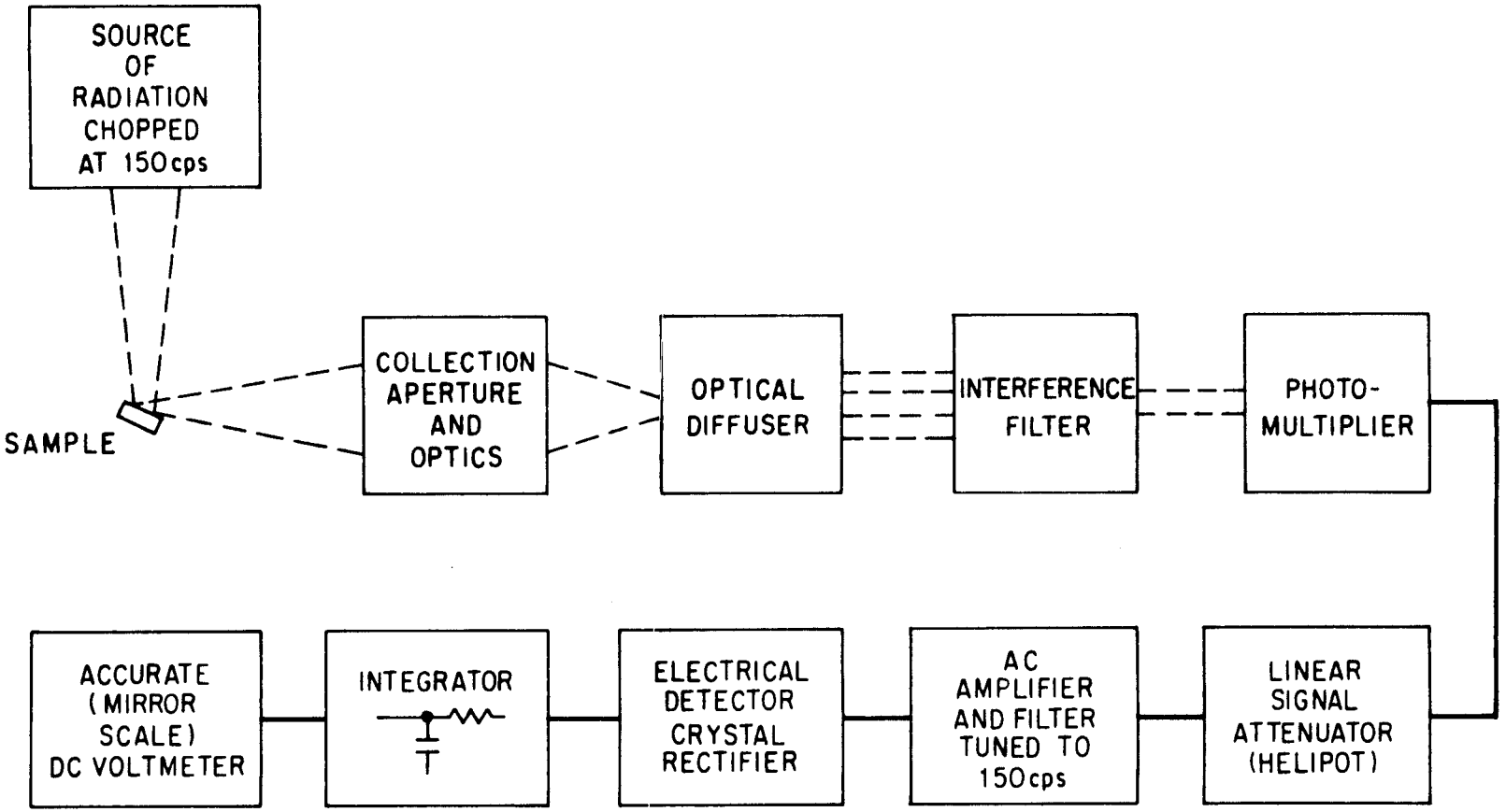

FIGURE 3 - FUNCTIONAL BLOCK DIAGRAM

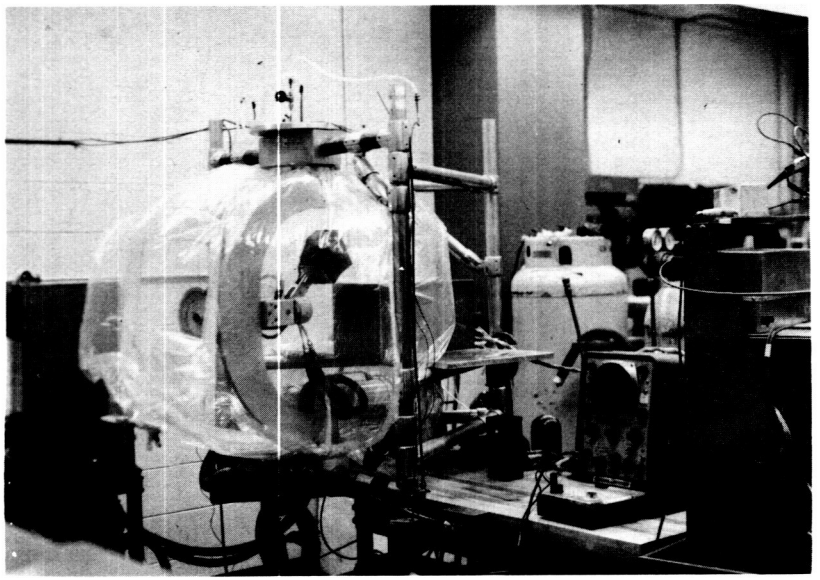

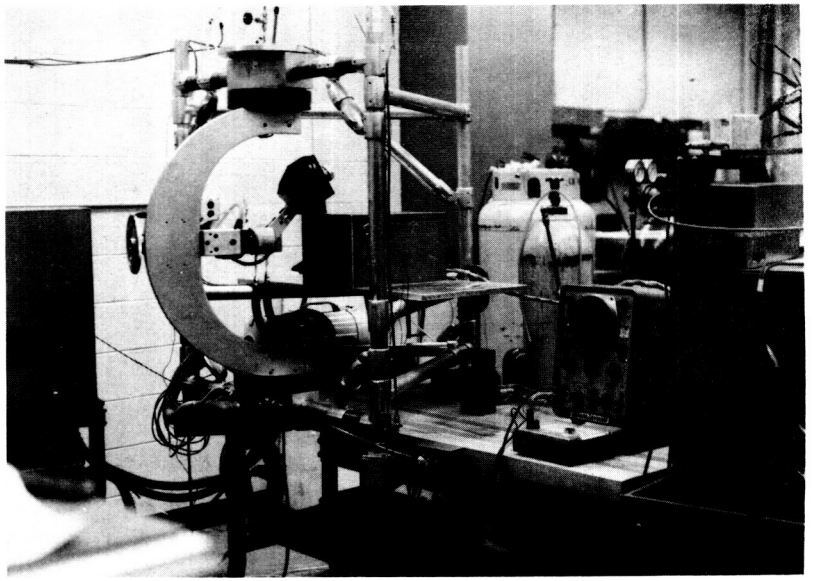

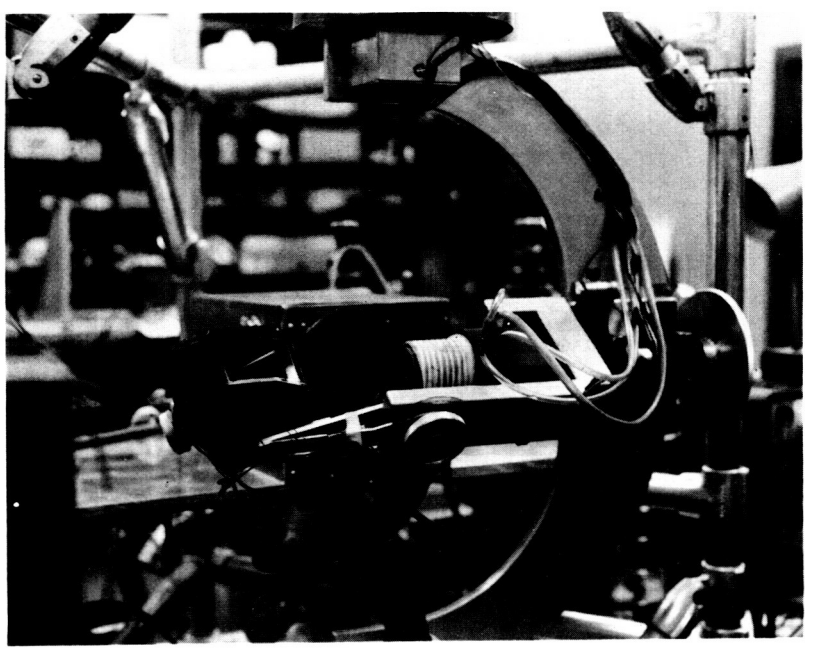

FIGURE 4 - REFLECTANCE APPARATUS

For hot-sample reflectance, the rf heater was turned up smoothly in about one minute to a power setting which usually could be left fixed through the run. The brightness temperature of the sample was read with a manually operated optical pyrometer three or more times during a run. Otherwise, the measuring procedure was the same as for cold runs.

Two men operated the equipment. One set angles read from a table, and for high temperature operated the rf unit and read sample temperatures. The other man took readings by setting a Helipot to any convenient value that brought the output voltmeter reading within $\pm$ 20% of a customary operating level and then recording the Helipot setting, the voltmeter reading, and the collection angles. (A typical data sheet is shown in Appendix D.) A single reflectance measurement, or run, usually took 20 minutes for a cold sample and one hour for a hot sample.

Reflectances were computed from the data sheets on a DEC PDPI computer located in a nearby firm (Bolt Beranek and Newman, Inc.) via teletype. The computing steps were as follows:

1. Obtain true readings from the voltmeter readings and Helipot settings for each of the 22 angular positions and the 2 incident readings.

2. Carry out an extrapolation.

3. Perform a summation.

4. Compute the reflectance.

D. PERFORMANCE AND ERRORS

Values such as reflectance or wavelength are expressed in decimal numbers; errors and differences are expressed as percentages.

The present equipment measures directional spectral reflectance ($R_{\psi \lambda T}$) of a flat sample at a temperature T, as stated below. Possible extensions of the performance are discussed under "Recommendations" in Section IV.

1. Angle ψ

Measurements can be made at any angle ψ between the limits of 33° and 72° (from the normal to the sample) and with a maximum error of $\pm$ $1/2^{\circ}$. This error in angle causes negligible error in the measurements.

2. Wavelength

The measurement wavelengths are as follows:

UV:	0.20 micron	12½% bandwidth
Blue:	0.40 micron	4½% bandwidth
Red:	0.65 micron	3½% bandwidth
IR:	1.00 micron	2½% bandwidth

The maximum uncertainty in the central wavelength is ± 1/2%. This error in wavelength causes negligible error in the measurements. The transmission at other than the central wavelength was negligible. The central wavelengths were set by interference filters purchased commercially.

3. Temperature

The temperature range within which satisfactory reflectance measurements can be made depends on the reflectance of the sample and on wavelength. For a char the range is as follows (average char temperature):

UV:	room temperature to 1575°C (2865°F)
Blue:	room temperature to 1285°C (2345°F)
Red:	room temperature to 1230°C (2245°F)
IR:	room temperature to 1100°C (2010°F)

For the sake of uniformity of data, measurements were not made at all four upper temperature limits, but at a lower compromise temperature corresponding to the red limit (see Section III).

The center of the char was cooler than the edge by an average 55°C (100°F), with considerable variability from sample to sample. The "average char temperature" is the numerical average of center and edge temperature. The standard deviation of a series of center readings on one char during a run was 20°C (35°F); this was due to variations of eye averaging of the radiancy, on a microscopic scale, of the pore structure of the sample. There appeared to be no recognizable constant increase or decrease of char brightness temperature during a run. The graphite holder was hotter than the edge of the char sample by an average difference of 250°C (450°F). We estimated the precision of our optical pyrometer readings (for example, on a constant-temperature blackbody) to be 5°C (10°F).

The over-all errors and differences in char temperatures almost certainly can be expected to cause negligible errors in reflectance.

4. Sample Oxidation at High Temperature

Heating chars in argon in this apparatus produces a substantial and permanent change in the sample. During a 1-hour high-temperature run the char changes in appearance from a graphitic grey to a velvety black, and its reflectance drops correspondingly. The porous structure also appears to become more tenuous. A special experiment showed the final hot reflectance at the end of a run to be about 14% of the initial cold value. When the sample is cooled this low value remains.

Examination of one of the samples at JPL showed that the blackened sample probably was oxidized. The effect seems to be a surface effect, not gross removal of char, although the corner of the initially cylindrical char does become rounded.

If oxidation is a primary factor in blackening, the cause of oxidation is not entirely clear. Two possible explanations are: first, that the sample undergoes some internal change, for example reaction with oxygen absorbed on its own surface. Secondly, sufficient oxygen may be contained in the argon atmosphere surrounding the sample to oxidize it. Discussion of theory of the argon-filled bag is included in Appendix C.

The argon used to fill the bag (as received in the tank) is Matheson ultra pure ionization grade (99.999%) and has the following analysis:

O_2	5 ppm
N_2	5 ppm
CH_4	2 ppm
CO	1 ppm
CO_2	1 ppm
H_2	1 ppm
H_2O	3 ppm

The filling procedure is to collapse the bag from its inflated volume of 15 cubic feet to 5% of this value and then to reinflate to the full 15 cubic feet again. Calculations show that with no air leaks in the bag after four such collapse and refill cycles, the purity of the final fill is approximately that of the 99.999% argon itself. The theory assumes proper mixing of new and old gas as the bag is reinflated. In this apparatus thorough mixing is accomplished with a mixing jet mounted in the bag which entrains and recirculates bag argon as it adds new argon. The effect of leaks in the bag is reduced to a low level by operating the bag at positive pressure for all but a brief portion of its fill cycle and by further minimizing the negative pressure phase of the later fill cycles.

A rough estimate of the effectiveness of the bag can be made by working backward. Assume that the sample is being oxidized and calculate how much oxygen would have to be present to cause this oxidation. Such reasoning shows that for the least oxidized samples corresponding to the most meticulous argon flushing there appears to be oxygen enough in the tank argon alone (5 to 10 ppm) to account for the observed sample oxidation without the necessity of postulating air leaks in the bag. Some of the samples showed greater oxidation and in the worst case suggested an oxygen level in the bag of 100 ppm and the possibility of small leaks. Sample blackening is also discussed in Section III, Results.

5. Over-all Error in Reflectance

Of the 75 measured reflectance values (runs), 51 represent more than one measurement at the same angle, wavelength, temperature (room), and sample, and can be used by appropriate small-sample techniques to estimate a standard deviation (precision). Accuracy is estimated by adding various estimated system errors one way and adding to this two times the standard deviation (see Appendix E, Discussion of Errors).

The figures below are estimates of absolute accuracy based on the above method and estimates of precision based on the data.

Cold Sample	Accuracy	$\pm$ 16% of reflectance
	Precision (σ)	$\pm$ 5% of reflectance
Hot Sample	Accuracy	$\pm$ 20% of reflectance
	Precision (σ)	$\pm$ 5% of reflectance

These figures apply to values of reflectance between 0.01 and 1.00. It is characteristic of this apparatus that accuracy and precision are approximately a constant fraction of reflectance down to a very low value of reflectance, less than 0.01. The accuracy and precision are unbiased, in that given a new single measurement of reflectance on an unknown material on this apparatus the most probable true value of reflectance is the measured value $\pm \sigma \approx 5\%$.

The statement of accuracy for hot samples characterizes the measuring technique itself, and does not include changes in the sample during measurement.

One remark should be made on our conclusions as to the significance of tendencies in the data before examining the data in detail. A slope in a fitted curve suggests a conclusion as to a tendency in the data. The significance of the conclusion depends on the number and scatter of the data points. Where one point only at each angle defines a curve, we are hardly justified in attaching significance to a tendency to within much narrower limits than the precision σ. On the other hand, if a cluster of several points defines an average value through which the curve is drawn at one angle, then we are justified in more refined conclusions. Specifically, for any one cluster of n data points at one angle, the standard deviation for the average--that is, the value of the curve at that angle--can be estimated to be the standard deviation of the population divided by the square root of n. For example, for a cluster of $n = 3$ points, the curve standard deviation might be estimated as $5\%/\sqrt{3} = 3\%$. In data such as we measured, where n is variable, often is 1, never is larger than 5, and where the extent of the scatter appears somewhat variable, subjective judgment is probably the best way of concluding that there is or is not a tendency present in the data. One applies what amounts to an intuitive regression analysis, bearing in mind that wherever more points are available a more specific conclusion can be drawn.

III. RESULTS

Our purpose was to learn as much as we could about two types of char samples within the limits of a reasonable number of reflectance runs and to verify our results qualitatively with a few measurements on other materials.

A. SAMPLES

JPL supplied prepared samples on which we made measurements as follows: two types of chars, coarse grained and fine grained; pyrolytic graphite; and Cat-a-lac black paint. These samples are described by JPL as shown in Table 1.

TABLE 1

TYPES OF SAMPLES

	Quantity	JPL Description
(Coarse)	18	40-50 Mesh furnace charred, then heat treated for 1 hour at 2500°C
(Fine)	39	80-100 Mesh furnace charred, then heat treated for 1 hour at 2500°C
	1	Pyrolytic graphite
	1	Cat-a-lac black paint disc

When received, both types of chars had already been pregraphitized by heating for 1 hour at 2500°C (under a pile of powdered graphite) to permit rf heating in our equipment.

The samples were in the form of 1/2 inch-diameter flat discs, and all were 1/10-inch thick except for the Cat-a-lac, which was received as a flat metal disc on which the Cat-a-lac had been painted.

The 40-50 mesh chars were fairly uniform char-to-char and appeared dark grey. On a microscopic scale this dark grey consisted of mottled silver grey plus black sponge-like pores.

The 80-100 mesh chars were not very uniform char-to-char in surface appearance. Many had three straight bands across the face--dark in the middle and silver-grey on either side--but some had very little banding.

For cold char reflectance measurements we selected one char of 40-50 mesh and one of 80-100 mesh, designated 40-50 Char III and 80-100 Char I, respectively. Each char was selected carefully to be representative of its batch, except that the 80-100 was selected to show a minimum of banding and also to have a representative mix of mottled silver grey and black (shown in a less uniform manner by many of the other 80-100 chars). Once mounted, each sample was left undisturbed in its graphite holder and whenever sample and holder was taken out of the apparatus and reinserted, they were remounted in the same position and angular orientation with respect to the apparatus.

Only the 80-100 mesh char was tested at high temperatures. A different char sample had to be used for each hot-reflectance measurement, because the surface and reflectance of the sample changed during a measurement.

Table 2 lists all the samples measured, our designations, the temperature of each, and the total number of measurements made.

B. MEASUREMENTS

In this program 75 individual values (runs) of directional spectral reflectance were measured: 55 on cold chars, 7 on hot chars, and 13 on other materials. All reflectance values measured in this program are given in Appendix A.

Measurements were made at four directional (incident) angles--$\psi = 33^{\circ}$ (near normal), 45°, 60°, and 72° (near glancing); at four wavelengths--0.20, 0.40, 0.65, and 1.00 micron; and at two temperatures, room and $2200^{\circ}F$. The 1.00-micron hot measurements were made at a lower char temperature, $2000^{\circ}F$, because of equipment limitations. At high temperature, as discussed earlier, the center of the char is cooler than the edge; the difference averaged $55^{\circ}C$ ($100^{\circ}F$) and varied from char to char.

There appears to be no clear way to plot all of the reflectance data that was measured in this program on one page. For this reason the data is divided into graphs of directional reflectance vs angle, one curve (or point) for each color and for each material that was measured (see Figures 5 through 10 and 12 and 13). These graphs contain all of the measured reflectance values and also show the scatter in individual values.

On each graph an average-value curve (or point) has been drawn, with only slight concessions to curve fitting, through the average value of real data points at each angle ψ. This average curve is used in Figure 14 as the basis for exhibiting the wavelength sensitivity (of the 45° reflectance) of all the materials.

TABLE 2

SAMPLES MEASURED

Quantity	Our Designation	Temperature	Number of Measurements
1	40-50 Char III	cold	9
1	80-100 Char I	cold	43
1	80-100 Char II	cold	1
7	80-100 Char random	hot	7
2	80-100 Char random	cold	2
1	Pyrolytic	cold	6
1	Cat-a-lac	cold	4
3	MgO (smoked)	cold	3
			75

Considering each figure in turn, we see in Figure 5 a graph of directional spectral reflectance $R_{\psi\lambda}$ of cold 40-50 mesh Char III versus directional angle ψ in the blue and also in the red. The char appears to have a slightly higher reflectance in the red than in the blue--6.3% at 45°, which (despite 5% over-all precision) is probably significant in view of the fact that the color difference exists at all four angles. There appears to be no significant trend in reflectance with directionality of this sample. As the angle goes from near normal (ψ = 33°) toward glancing (ψ = 72°) the reflectance varies only by -3.8% in the blue and +3.7% in the red.

No further measurements were made on 40-50 char. Instead we concentrated on the finer grained 80-100 char.

Figure 6 shows the directional spectral reflectance of 80-100 mesh Char I vs angle in the ultraviolet. The most obvious trend is an increase of reflectance toward glancing angles, 14% from ψ = 33° to ψ = 72°. In view of σ = 5% precision, this trend is significant.

Figure 7 is a similar graph ($R_{\psi\lambda}$ vs ψ) showing cold reflectance of the same 80-100 Char I sample in the blue. The tendency toward increasing reflectance with angle is evident but too slight (5.4%) to be considered significant.

One additional material is included in Figure 7. To test the difference between two different samples of nominally identical 80-100 char, we picked a second char (designated 80-100 Char II) that looked similar to 80-100 I and also measured its reflectance cold at 45°, blue. As evidenced from the graph, the blue average of 80-100 Char I and the

value of the point for 80-100 Char II differ by some 19%.

Figure 8 is a similar graph for 80-100 I char in red. Reflectance increases 9.6% from $\psi = 33^{o}$ to 72^{o}.

Figure 9 plots $R_{\psi\lambda}$ vs ψ for 80-100 I in infrared. Reflectance increases 5.1%.

To summarize the angular sensitivity of the one 80-100 Char I sample tested, Figures 6 through 9 show a tendency toward increasing reflectance as the directional angle moves toward glancing. Averaged for all wavelengths, the tendency is 8.6% and can probably be considered significant. This averaged tendency, if extrapolated linearly, would give a 12½% difference between directional reflectance in the region of near normal ($\psi = 33^{o}$) and reflectance at $\psi = 90^{o}$.

Another tendency is just noticeably suggested in Figures 6 through 9: that the reflectance in the region of 33^{o} and 45^{o} is flat and, to extrapolate toward $\psi = 0^{o}$, that directional reflectance in the region between the pole $\psi = 0^{o}$ and $\psi = 45^{o}$ is approximately independent of angle ψ for the Char I sample.

High-temperature char reflectances were measured. As discussed earlier, the samples turn during heating from a graphite grey, porous-appearing surface to a velvety black during the course of a one-hour run and reflectance drops correspondingly. Since this change takes place progressively during the reflectance run, the meaning of the measured high temperature reflectance values is questionable.

Figure 10 shows the results of an experiment to characterize this change in the char with time. During the course of one of the high-temperature reflectance runs, a second experiment was conducted concurrently. One of the 22 collection angle positions was chosen as a monitoring position; periodically during the reflectance run, the operator briefly turned to the monitoring position, read signal and time, and then returned to the reflectance run. The angular position of this monitoring reading was chosen, on the basis of past experience with chars, to be relatively insensitive to the changes that could be expected in the shape of the photometric lobe during the one-hour run. The signal at the monitoring position is a relative (photometric) signal only, but plotted in this way it gives an idea of the relative change of reflectance of the sample with time.

The next step was to normalize all of the monitoring readings so that the normalized value of the first monitoring reading taken on the cold sample before heating equalled the cold reflectance before heating. The other (normalized) monitor readings would then be approximately equal at any time to the sample reflectance. Thus, these monitoring readings are estimated reflectance values and when plotted as in Figure 10 provide a curve of (estimated) sample reflectance as a function of time during a run.

Figure 10 shows estimated 45° blue reflectance vs time for one 80-100 char random sample during a high-temperature run and shows also the cold reflectance of the same sample both before and after heating. The over-all measured value of "hot reflectance" for the run is noted on the graph. The temperature of the char during the run is also noted; the dotted portion of the temperature history was estimated on the basis of the rf heater power, and the solid portion was based on optical pyrometer readings.

The decay curve of Figure 10 shows that the (estimated) sample reflectance drops to 50% of its initial cold value 5.5 minutes after the char reaches temperature, to 23.2% of its initial cold value in 28.7 minutes, and to 13.9% of its initial cold value in 63.1 minutes (the end of the run).

The point on the decay curve corresponding to 23.2% of initial cold reflectance also coincides with the over-all measured hot reflectance value for the run.*

The cold reflectance after heating was measured and, as indicated in Figure 10, was found to be approximately the same as the final (estimated) hot reflectance value before the sample was cooled.

When a char has been cooled down after a reflectance run, it is apparent that some char material has disappeared. One reasonable theory as to the cause of such erosion is oxidation by the surrounding atmosphere. The least eroded samples show observable erosion of the char that corresponds with the amount of oxidation that might be expected from the tank argon alone (5 to 10 ppm) without postulating air leaks in the bag. The most eroded (oxidized) samples correspond to an oxygen level in the bag in the range of 100 ppm. Further, the removal of material is slightly more noticeable at the bottom of the vertical char face than elsewhere; this could be the result of convective flow up past the hot sample.

On the theory that oxygen might be leaking into the bag and causing oxidation, an attempt was made to shield the sample from bag argon by the use of a gentle laminar flow of high-purity (99.999%) argon out from behind and around the sample. This arrangement did not stop sample blackening, but did change the pattern of sample erosion. Now the outside corner of the disc was rounded off evenly around the disc perimeter. Again, the amount of material removed corresponded in order of magnitude to the amount of oxygen that would be delivered by the laminar argon flow from behind the sample. If oxidation is taking place, a reasonable way of preventing it would be to place a chemical getter in the bag before and during the hot run.

---

*Note the time scale of Figure 10; the sample first reaches temperature at about t = 8.0 minutes on the abscissa.

One must bear in mind that the samples are changing during heating and that the composite reflectance value resulting from each run is therefore questionable. Nevertheless, the plotted values do show recognizable patterns.

Measured value of high-temperature char reflectance are plotted in Figure 11. Seven random samples of 80-100 char were heated to 2200°F and measured at 45° UV, 45° and 72° blue, 45° red, and 45° IR (at 2000°F). The figure suggests several tendencies in the data from these samples:

- The general level of high-temperature char reflectance is very much lower (by a factor of four) than the reflectances of cold char 80-100 I and 80-100 II which have not been heated.

- Two different samples at the same angle ($\psi = 45^{\circ}$) and wavelength ($\lambda = 0.4\mu$) show a 16-1/2% difference in hot reflectance.

- An angular tendency is suggested. The reflectance value at $\psi = 72^{\circ}$ is higher than either of the two reflectance values at $\psi = 45^{\circ}$ and 18.3% higher than the average of both.

- A spectral tendency is indicated (see also Figure 14). The 45° reflectances appear highest at the longest wavelengths. The difference between the highest 45° IR reflectance and the lowest of the average of two 45° blue reflectances is 25%.

The reflectance of cold pyrolytic graphite was measured. Figure 12 shows the directional spectral reflectance of this material (as received from JPL) for $\psi = 33^{\circ}$, 45°, 60°, and 72° in the blue and for $\psi = 45^{\circ}$ in the UV and red. The infrared reflectance was not measured.

The figure shows a marked angular sensitivity with increasing reflectance toward glancing angles. The difference between the 33° and 72° points on the curve is 30%. If extrapolated linearly in both angular directions, this slope leads to a glancing ($\psi = 90^{\circ}$) reflectance of 0.198, which is two times the normal reflectance (0.099).

This sample of pyrolytic graphite also shows a marked wavelength sensitivity, namely an increase of reflectance at the longer wavelengths (see also Figure 14).

Figure 13 shows measurements of MgO and Cat-a-lac black paint made at the closest available angle to normal, $\psi = 33^{\circ}$. To facilitate comparison, points are plotted on the same coordinate system as the char and pyrolytic graphite data, but measurements at only one angle were made. For MgO three points were measured in blue. The three points have a mean value of 0.957 with +5.3%, -5.2%, and -0.0% deviation (linear) from the average.

Four Cat-a-lac reflectances were measured (33^{o})--three at blue, one at red. The three blue values have a mean of 0.0546, with +0.4%, -3.4%, and +3.0% deviations (linear) from the mean. One more point is plotted, reflectance at (33^{o}) red. Cat-a-lac appears to show no significant wavelength sensitivity, since the red value differs from the average blue by only +3.6%.

Other data on Cat-a-lac compiled at JPL is included on Figure 13 for comparison.* A number of JPL data points for normal spectral reflectance of Cat-a-lac in the blue and red have an average value of .0475 and range from 0.04 to 0.05.

The foregoing Figures 5 through 13 complete the report of the measured data. The last Figure, 14, is based on the average values developed in the earlier figures. "Average value" in some instances is based on one point. Figure 14 summarizes the wavelength sensitivity of five materials: cold 40-50 Char III, cold 80-100 Char I, hot 80-100 Char random, cold pyrolytic graphite, and cold Cat-a-lac. The plots show average values of 45^{o} directional reflectances versus wavelength, except for one curve that shows 33^{o} reflectance for Cat-a-lac.

The wavelength sensitivity of the materials shown in Figure 14 can be characterized by labeling each with a "color" by analogy to visual perception. On this basis, the pyrolytic graphite could be called a "red" material. The others (cold 80-100 I, cold 40-50 III, and random hot 80-100) could be called approximately "grey" materials.

---

* Communicated by R. Nagler of JPL.

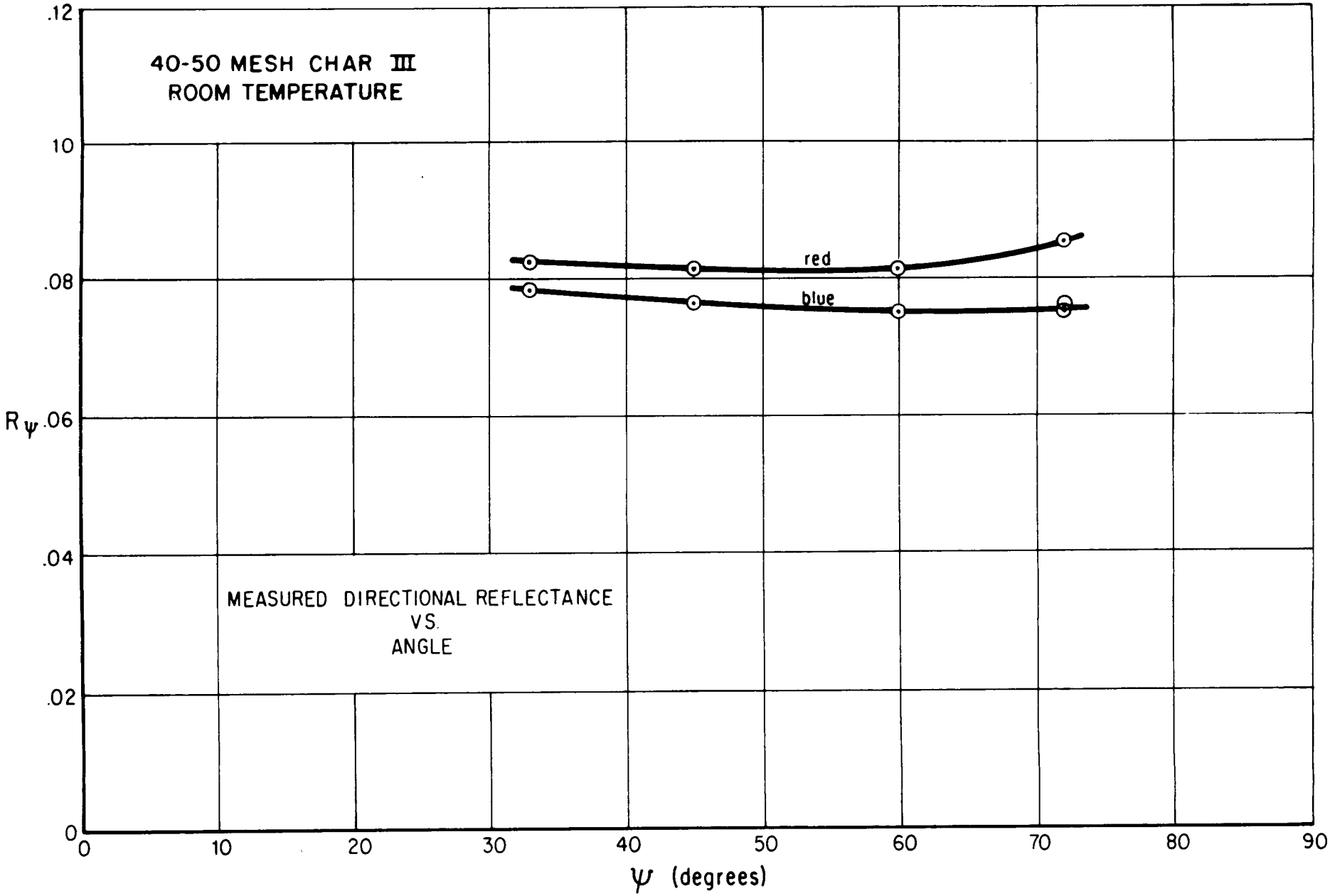

FIGURE 5 - COLD REFLECTANCE OF 40-50 MESH CHAR III

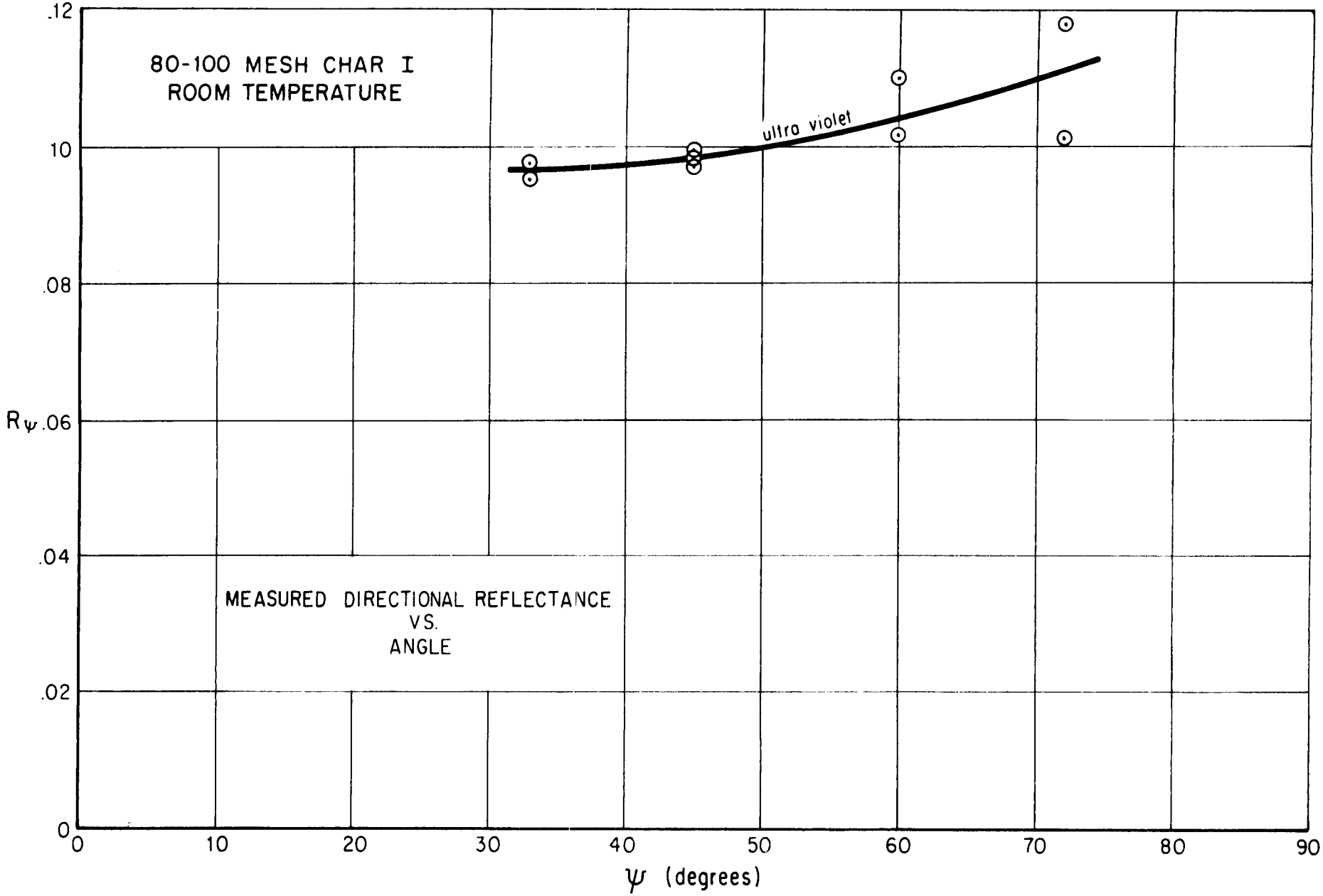

FIGURE 6 - COLD REFLECTANCE OF 80-100 MESH CHARS I -- UV

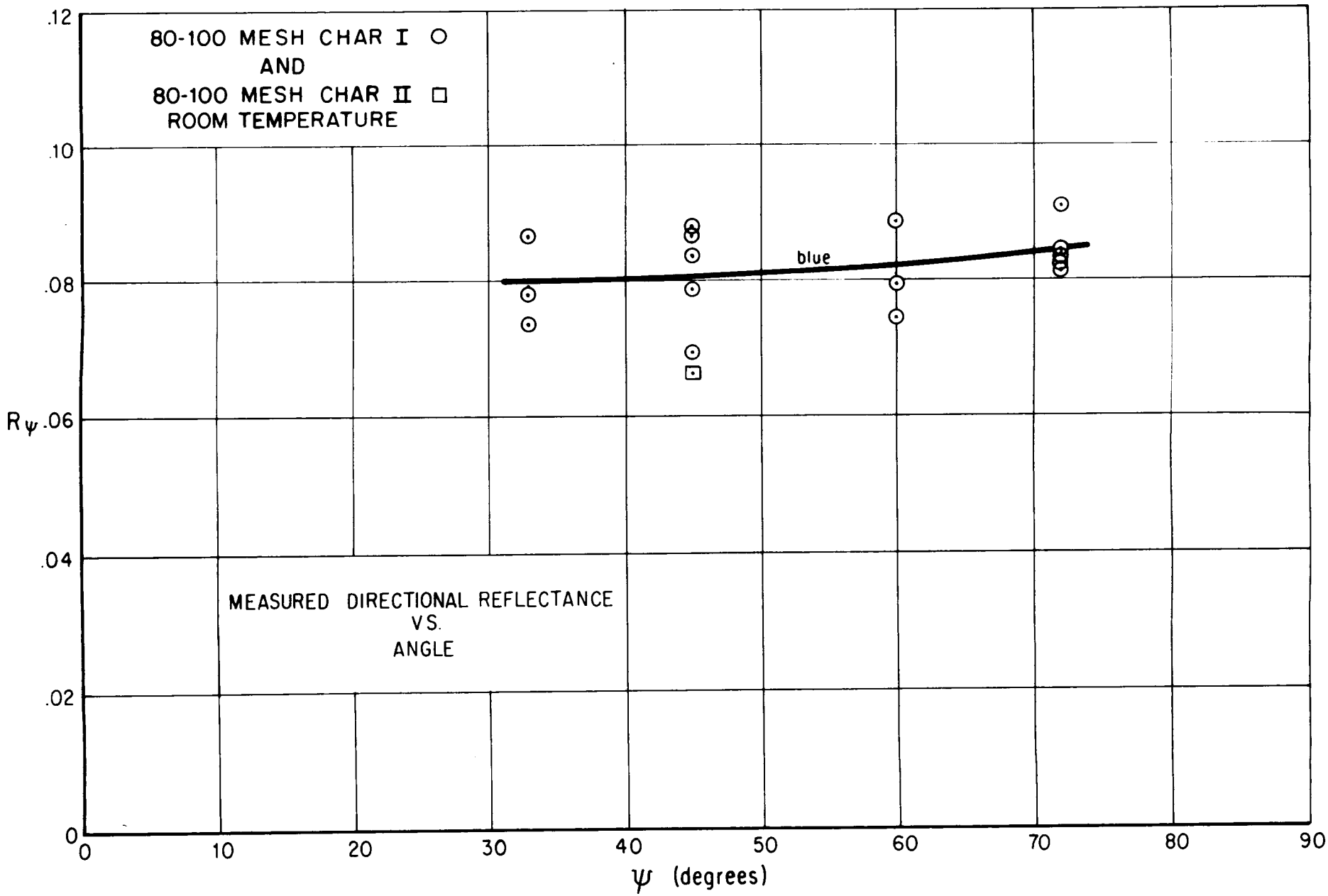

FIGURE 7 - COLD REFLECTANCE OF 80-100 MESH CHARS I AND II -- BLUE

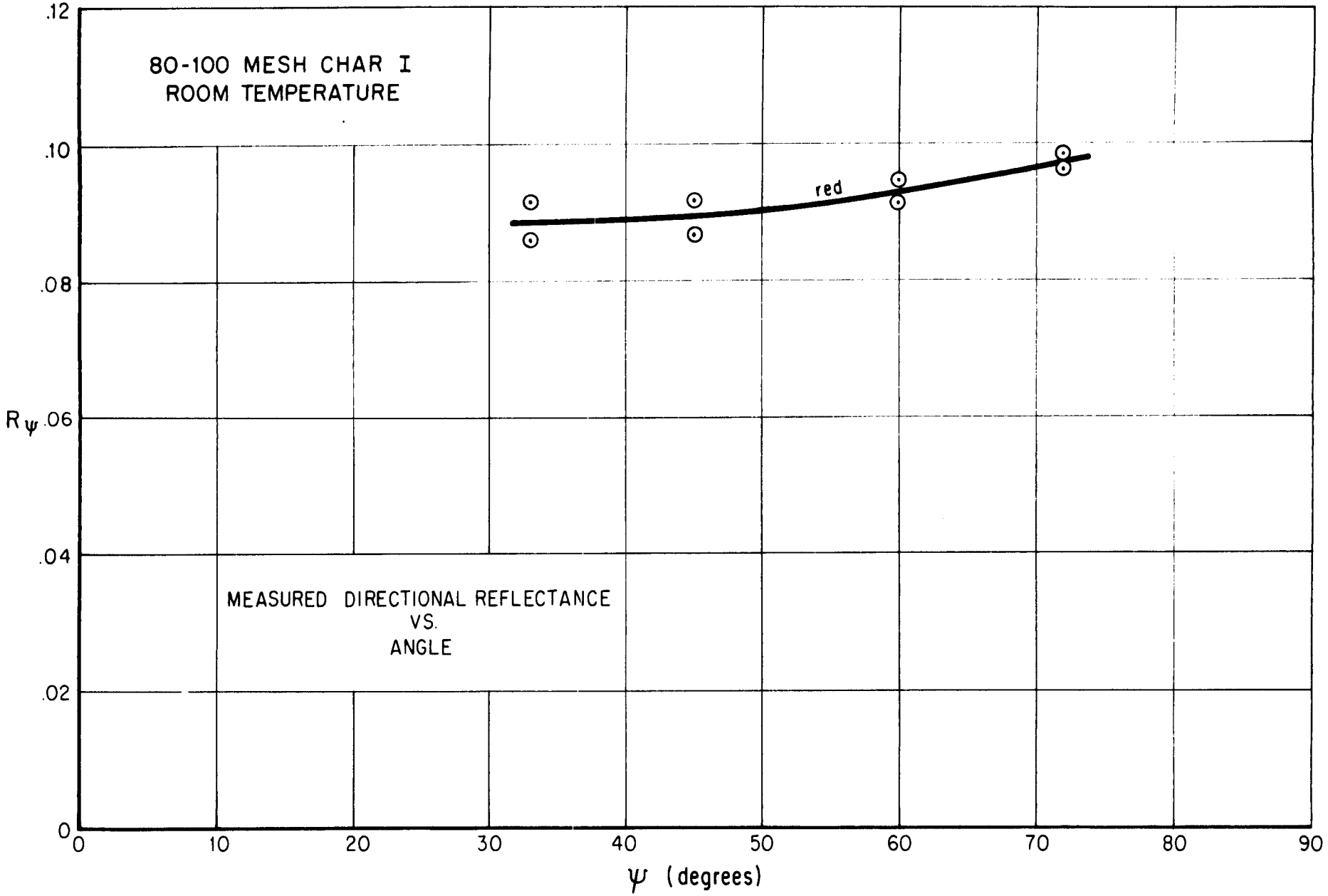

FIGURE 8 - COLD REFLECTANCE OF 80-100 MESH CHAR I -- RED

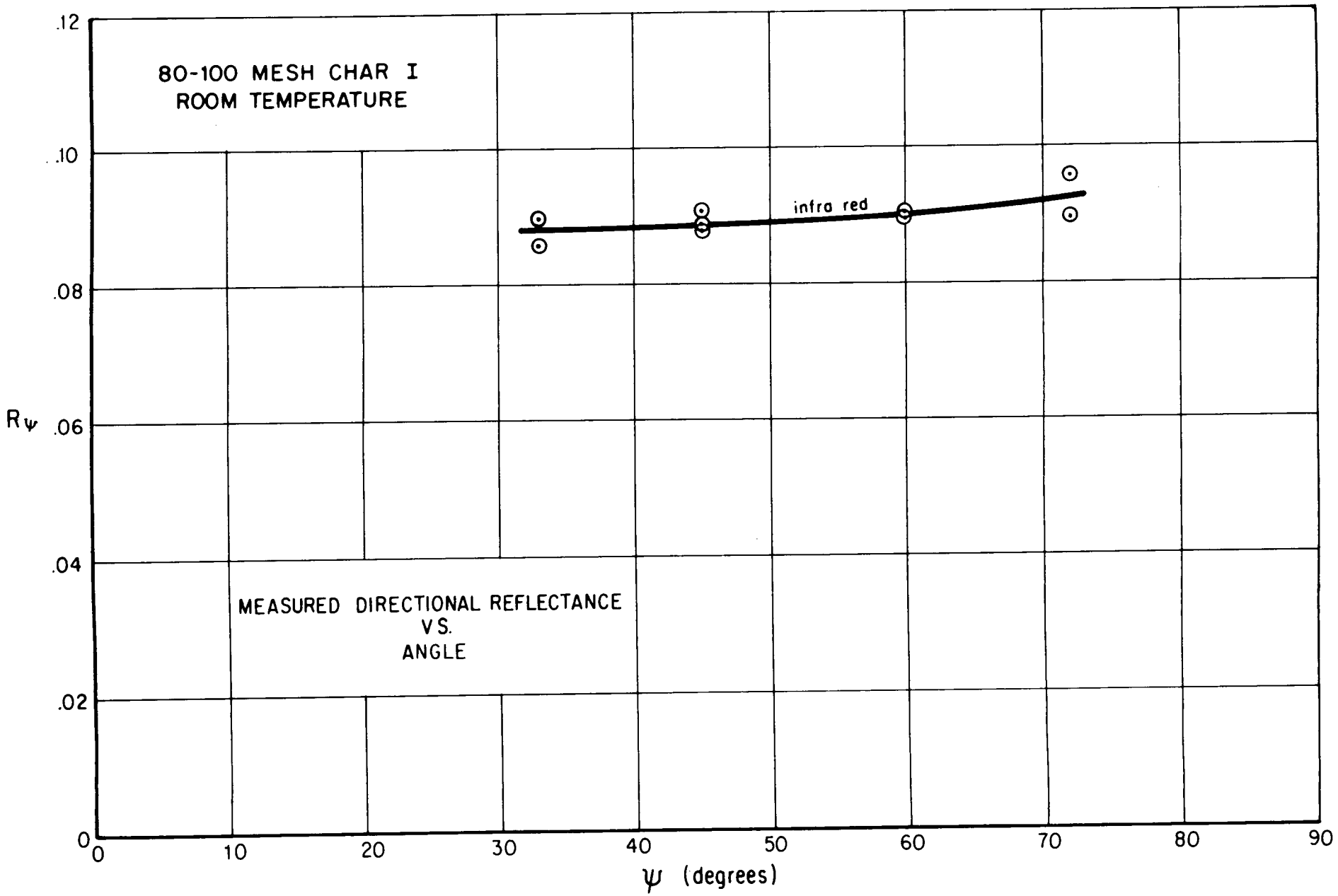

FIGURE 9 - COLD REFLECTANCE OF 80-100 MESH CHAR I -- IR

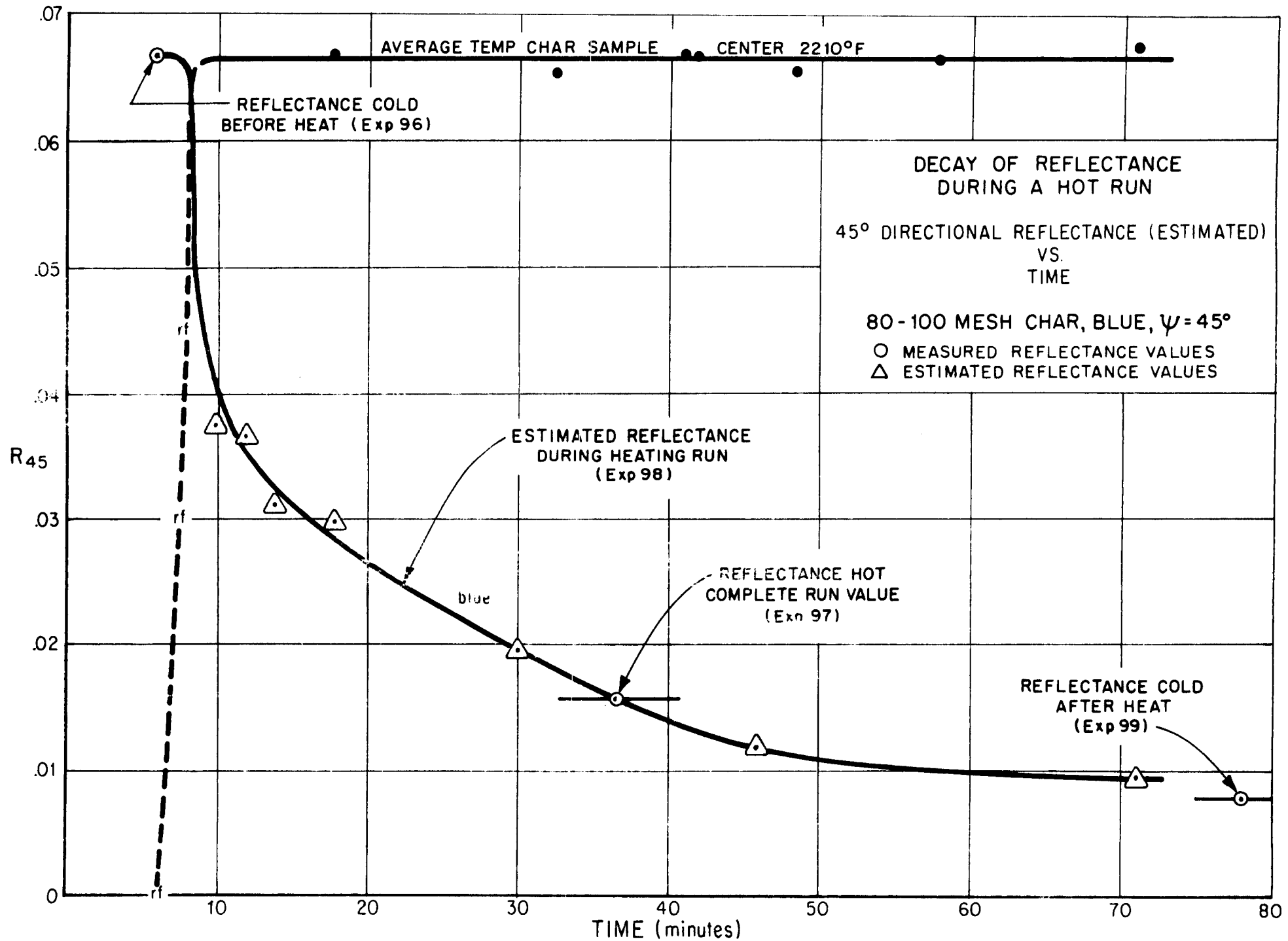

FIGURE 10 - DECAY OF REFLECTANCE DURING A HOT RUN

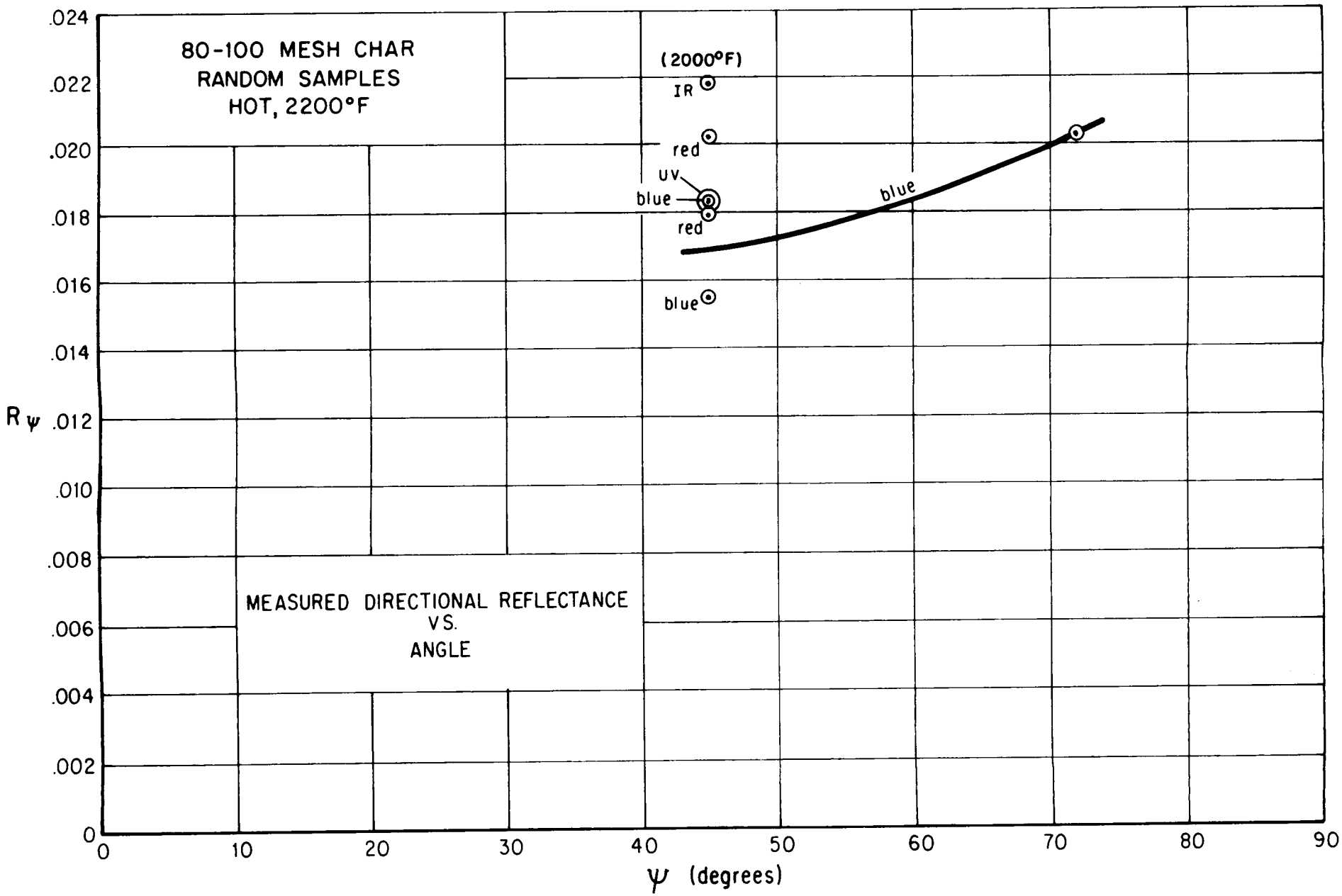

FIGURE 11 - HOT REFLECTANCE OF 80-100 MESH CHAR

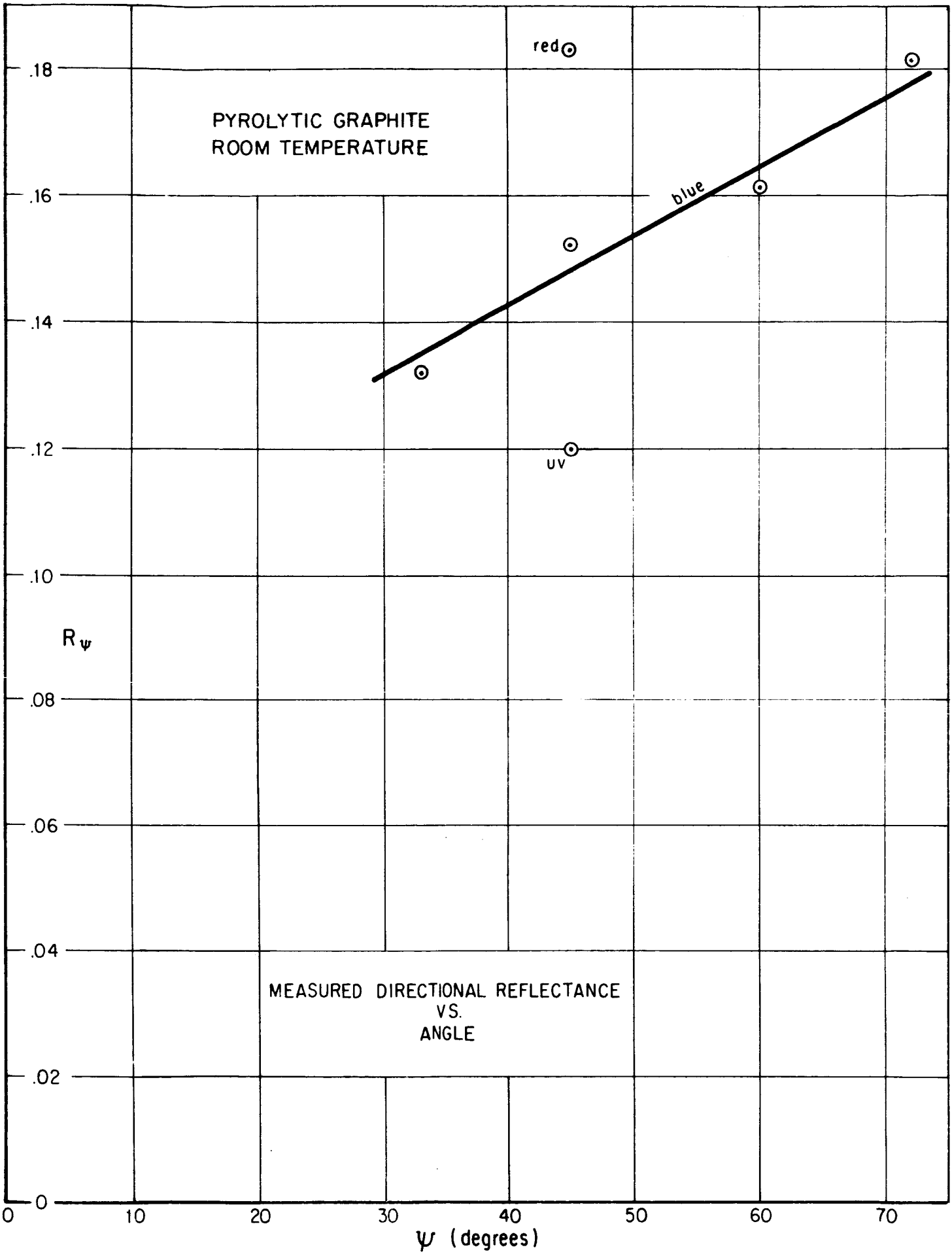

FIGURE 12 - COLD REFLECTANCE OF PYROLYTIC GRAPHITE

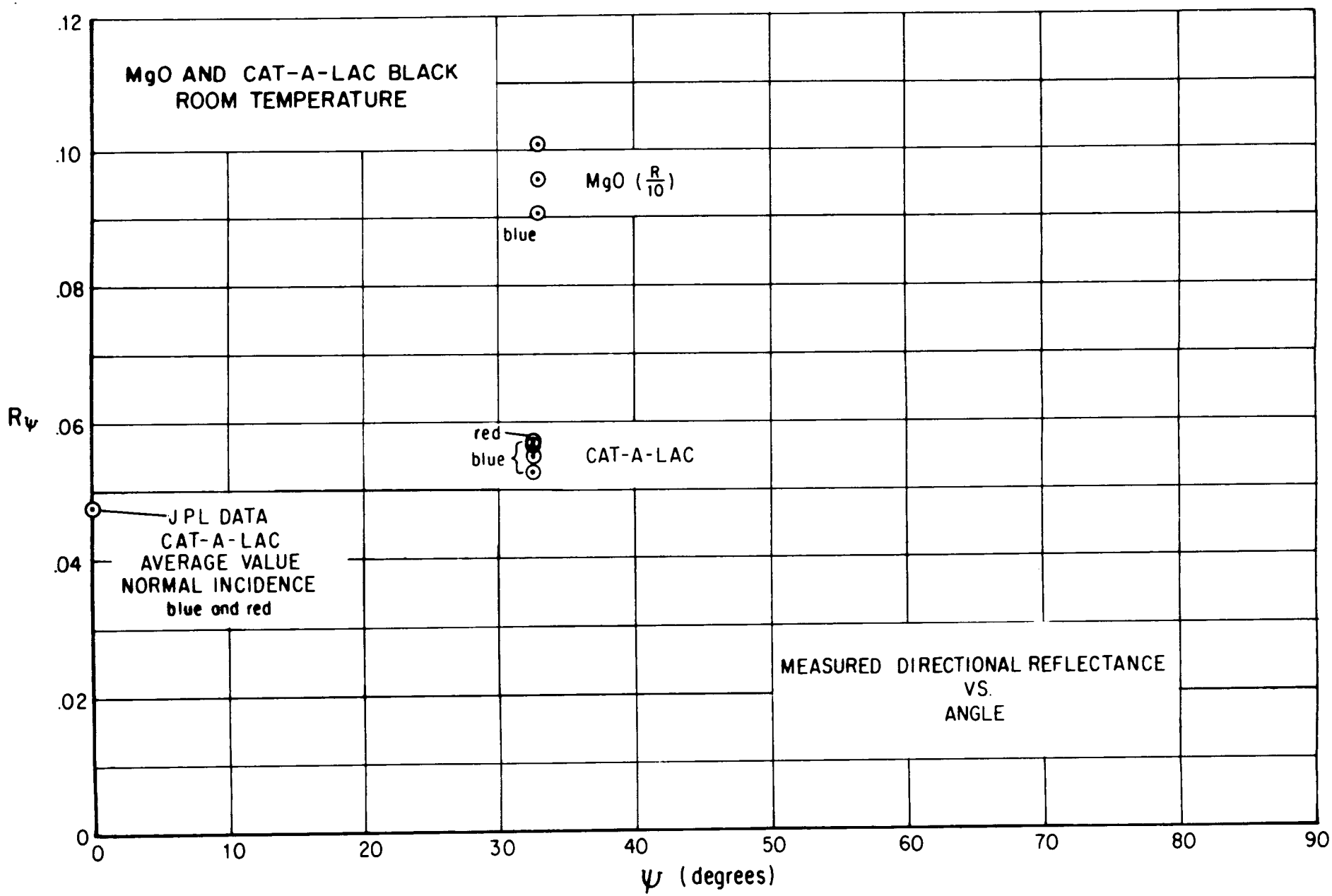

FIGURE 13 - COLD REFLECTANCE OF MgO AND CAT-A-LAC BLACK

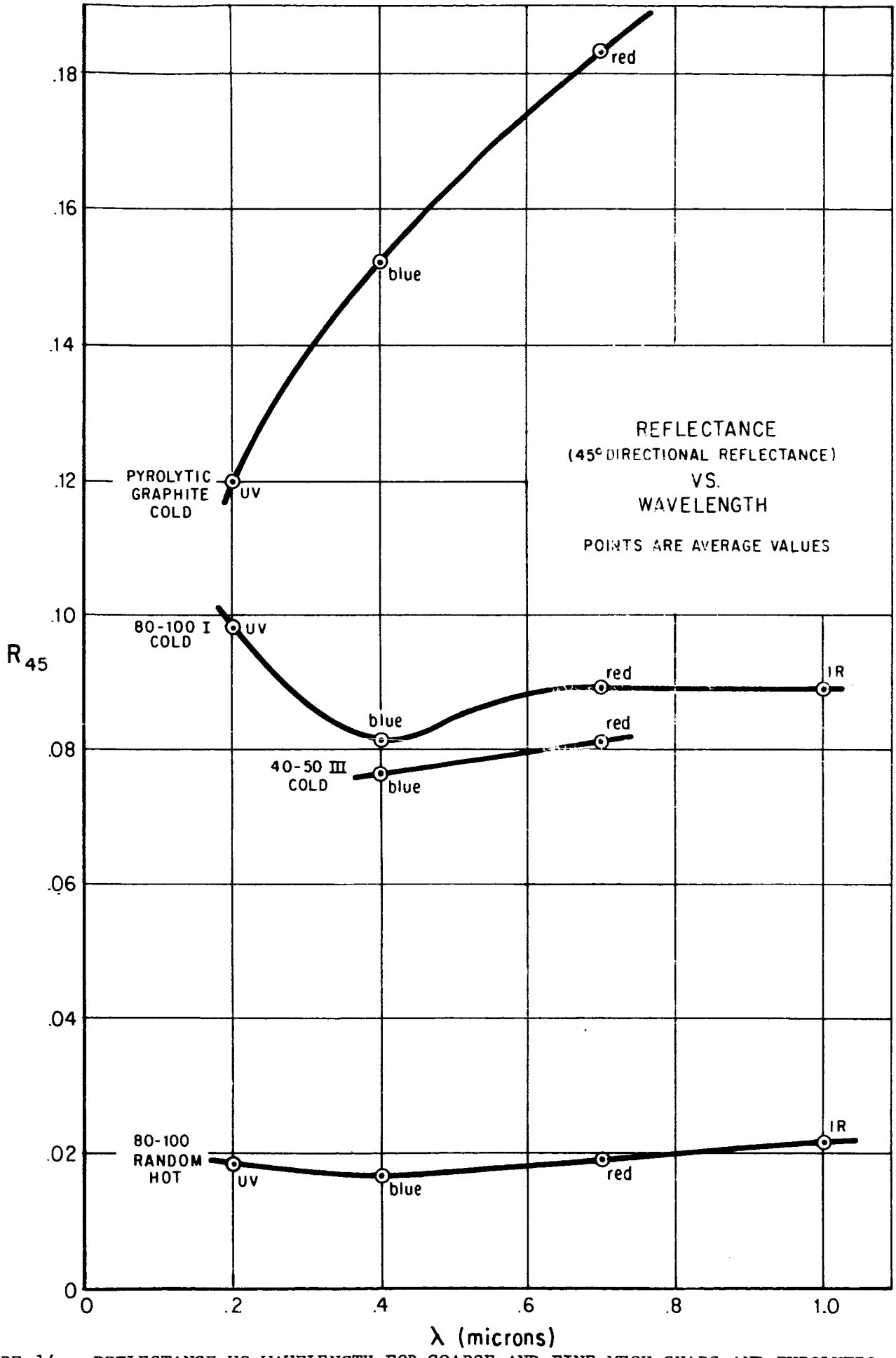

FIGURE 14 - REFLECTANCE VS WAVELENGTH FOR COARSE AND FINE MESH CHARS AND PYROLYTIC GRAPHITE

IV. CONCLUSIONS

1. The three-dimensional goniometric reflectance technique proved to be a satisfactory and fundamentally reliable method for measuring directional spectral reflectance. The present capabilities are angles from 33° to 72°, wavelengths from 0.2 micron to 1.0 micron, and temperatures from room temperature to 2200°F (ignoring the problem of sample change at high temperature).

2. Changes in samples during a high-temperature run proved to be a major problem. Samples were converted from a graphite-grey disc to a velvety black surface during the course of measurement. The cause of the change is not known. One explanation is that the surrounding argon contained traces of oxygen, which caused the hot samples to blacken; this oxygen could have come either from trace quantities in the argon supply or entered through one or more very small air leaks in the atmosphere bag surrounding the samples.

3. Reflectance measurements were made at four angles: 33°, 45°, 60°, and 72°; at four wavelengths: 0.2μ, 0.4μ, 0.65μ, and 1.0μ; and at two temperatures: room and 2200°F. Seventy-five measurements were made, 55 on cold chars, 7 on hot chars, and 13 on other cold materials--pyrolytic graphite, Cat-a-lac black paint, and MgO.

Measured reflectances for the cold chars ranged from 0.07 to 0.10, depending on angle and wavelength. The coarser grained char (40-50 mesh) ran slightly lower in reflectance (5 to 10%) than the finer grained char (80-100 mesh).

4. In general, the char's directional spectral reflectances were relatively independent of angle and of wavelength; each exhibited variation in the order of 1/10th reflectance value over the angles and wavelength ranges.

5. The difference in reflectances between two nominally identical char samples was 20%.

6. Hot chars showed a much lower reflectance than cold, by a factor of four, due primarily to sample change during measurement.

7. Cold pyrolytic graphite shows a substantial sensitivity of reflectance, both to angle and to wavelength; its reflectance increases with glancing angles and longer wavelengths.

8. Cat-a-lac black paint was measured at a near-normal angle (33°) at 0.4 micron and had an average reflectance value of 0.0546.

V. RECOMMENDATIONS

1. A three-dimensional goniometer of the type used in this program is a reliable and accurate device for determining absolute reflectance and is applicable to a wide variety of reflectance problems, on cold or hot materials.

2. The method is absolute; reflectance is determined only from ratios of readings and from the geometry of the apparatus. It does not depend on the reflectance of any secondary reflecting surface, nor does it require any reflectance standard. For the foregoing reasons this goniometric method should be considered for measuring (calibrating) materials that are to be used as reflectance standards.

3. For future applications, the apparatus described in this report may be readily refined in accuracy and extended in angle, wavelength, and temperature. Also, the atmosphere, which may have had a chemical effect on hot samples, may be purified.

a. Accuracy. The accuracy and precision of the apparatus used in the present program have been governed by the behavior of certain components, by the larger random errors arising in data taken earlier in the program (before the experimental technique had been refined), and by the necessity for obtaining a considerable quantity of data in a limited time. Refinements, such as the use of a better diffuser and a-c amplifier, would improve accuracy and precision by a factor of two or more.

b. Angle. The present range of incident angles is from 33° to 72° (measured from the normal to the sample). The limits of this range are defined by mechanical interference and considerations of incident beam width. However, the range may be increased to any extent desired by appropriate redesign of the source and collecting apertures and housings. A practical initial step would be to extend the range of incident angles to 15° - 75°.

c. Wavelength. The goniometric method is potentially applicable over a very wide wavelength range, from 0.2 micron to 200 microns. The ease or difficulty of measurement in any particular wavelength region will depend on the performance of the best available detector and its signal-to-noise ratio. Initially, it would be practical to extend wavelength to a range of 0.2 micron to 3 microns using photomultiplier and lead sulfide detectors.

d. Temperature. The maximum operating temperature of the apparatus used in this program depends on the wavelength of the incident beam; at any given wavelength it depends on the performance of the radiant source and the signal processing components. Higher temperatures are possible by refinement of these components. An initial extension to $3000^{\circ}F$ would be practical.

e. Atmosphere. The large reflectance changes that were observed in hot char samples during measurement may be caused by oxidation. If so, and if oxygen is being introduced into the atmosphere bag, either as an impurity in the argon or via leaks in the bag, it could be quite easily removed by placing chemical getters inside the bag. At least as a precaution, getters should be used in any high-temperature measurements of materials known to react with oxygen.

APPENDIX A

REFLECTANCE DATA

Table A1 lists all the reflectance values for all the materials that were measured in this program.

The original data on which these values are based is contained in two data books on file at Arthur D. Little, Inc. under Case No. 66658. These books contain a pair of original data sheets (pages 1 and 2) for each reflectance value shown in Table A1. Each pair of data sheets was assigned an experiment number at the time the reflectance was measured, and this number appears to the left of the reflectance value. Where measurements were made at more than one angle (e.g., 80-100 I at UV at $\Psi = 33^{o}$, 45^{o}, 60^{o}, and 72^{o}), the related pairs of data sheets are identified by letters A, B, C, or D added to the experiment number.

TABLE A1

DIRECTIONAL SPECTRAL REFLECTANCE

Material	Temp.	UV, .20μ Exp. No.	UV, .20μ 33°	UV, .20μ 45°	UV, .20μ 60°	UV, .20μ 72°	Blue, .40μ Exp. No.	Blue, .40μ 33°	Blue, .40μ 45°	Blue, .40μ 60°	Blue, .40μ 72°	Red, .65μ Exp. No.	Red, .65μ 33°	Red, .65μ 45°	Red, .65μ 60°	Red, .65μ 72°	IR, 1.00μ Exp. No.	IR, 1.00μ 33°	IR, 1.00μ 45°	IR, 1.00μ 60°	IR, 1.00μ 72°
40-50 III	Cold						56	.0785	.0765	.0752	.0760										
							58				.0754	65	.0823	.0813	.0816	.0854					
							57	.0779	.0788	.0797	.0833										
80-100 I	Cold																				
							59				.0820										
		72		.0993			60				.0837	64	.0859	.0868	.0912	.0961	68	.0857	.0886	.0902	.0955
		73	.0978	.0981	.1099	.1178	76	.0735	.0691	.0745	.0817						69		.0906		
		74		.0971			79		.0879												
		85	.0951	.0977	.1019	.1011	80	.0864	.0865	.0885	.0904	81	.0916	.0919	.0948	.0984	83	.0894	.0881	.0895	.0895
							103		.0839												
80-100 II	Cold						96		.0668												
80-100 (random)	Cold						95		.0147												
							99		.0077												
80-100 (random)	Hot						93		.0183			91		.0179							
							94				.0203	92		.0202							
		106		.0183			97		.0155								105		.0218		
Pyrolytic Graphite	Cold	108		.1198			110	.1320	.1523	.1615	.1818	111		.1832							
MgO	Cold						55	1.008													
							102	.907													
							112	.956													
Cat-a-Lac black paint	Cold						62	.0548				63	.0566								
							77	.0527													
							101	.0562													

APPENDIX B

METHOD OF MEASUREMENT

A. DEFINITION OF REFLECTANCE

The reflectance measured in this apparatus is directional spectral reflectance, defined as the ratio of all radiation reflected from the sample in a specified wavelength band to all radiation incident onto the sample in the same wavelength band, with the incident radiation confined to a narrow beam.

The directional spectral reflectance determined in this way is related to the corresponding quantities directional spectral absorptance and directional spectral emittance. A clear statement of these relationships, particularly with regard to angle, is given by Richmond*.

B. COORDINATE SYSTEM

The polar coordinate system of this apparatus is shown in Figure 1 (which is repeated in this appendix for convenience). The sample is located at the origin of the spherical polar coordinate system, and the coordinate system remains fixed with respect to the sample; specifically, the normal line through the center of the sample passes up through the pole of the coordinate hemisphere above it, and the plane of the flat (reflectance) face of the sample coincides with the base plane of the coordinate hemisphere.

A narrow beam of radiation is incident on the center of the sample. This beam has two angular coordinates. The vertical angle of the incident beam is measured from the pole of the coordinate hemisphere and is labeled the zenith angle ψ . The incident radiation has an azimuthal angle (labeled "A_z" or 0^o) that is always zero by definition; i.e., the azimuthal angle of any location around the hemisphere is measured from a zero defined by the vertical plane containing the incident beam.

A beam of radiation is collected from the sample. The collected beam has two angular coordinates. The vertical angle of the collected beam is measured from the pole of the coordinate hemisphere and is labeled the zenith angle ϕ . The collected radiation has an azimuthal angle θ measured from the plane of the incident beam.

---

* Joseph C. Richmond, "Physical Standards of Emittance and Reflectance", a paper in Radiative Transfer from Solid Materials, Blan and Fischer eds., New York, Macmillan, 1962.

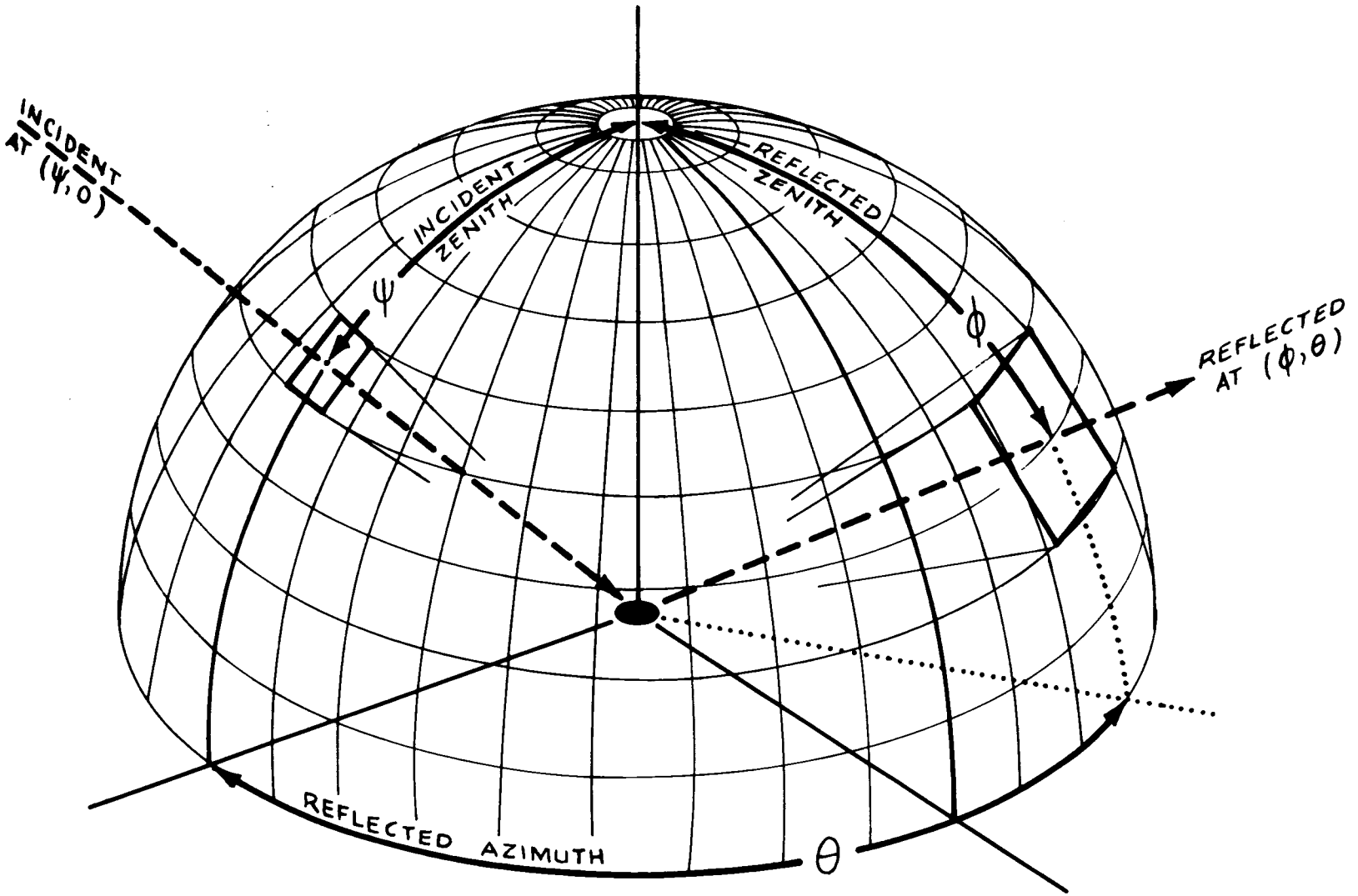

FIGURE 1 - REFLECTANCE COORDINATE SYSTEM

When a location on the coordinate hemisphere is specified, the polar (vertical) angle is stated first and the horizontal angle second. Thus, coordinates will be:

$$\text{Incident beam} \quad (\Psi, \ 0)$$

$$\text{Reflected beam} \quad (\phi, \ \theta)$$

For example, the incident and reflected beams shown in Figure 1 are:

$$\text{Incident} \quad (\Psi, \ 0) = (45^{\circ}, \ 0^{\circ})$$

$$\text{Reflected} \quad (\phi, \ \theta) = (60^{\circ}, \ 120^{\circ})$$

The maximum quadrant limits of these angles will be:

$$\text{Incident} \begin{cases} \Psi : 0^{\circ} \text{ to } 90^{\circ} \\ A_z : 0^{\circ} \end{cases}$$

$$\text{Reflected} \begin{cases} \phi : 0^{\circ} \text{ to } 90^{\circ} \\ \theta : 0^{\circ} \text{ to } 180^{\circ} \end{cases}$$

The limits of the measuring apparatus are somewhat less, due to interference between source and collector optics.

C. SOURCE AND COLLECTOR

The source of incident radiation is a small housing containing a front-surfaced paraboloidal mirror, a flat mirror, an 1800-rpm hysteresis synchronous chopping motor, a chopping disc with five evenly spaced holes, and a radiation source. The radiation source may be either 1) a Hitashi Nitora tungsten lamp (10V, 4A) overdriven to 12 or 14 volts or 2) a Hannau Model D102B deuterium lamp operating at 30 watts. The deuterium lamp is used for UV, the tungsten for blue, red, and IR measurements.

The incident beam emerging from this source has the shape of a narrow rectangular cone focused down onto the sample. The size of the cone is:

$$\Delta\Psi = 9.5^{\circ}$$

$$\Delta A_z = 9.9^{\circ}$$

The incident beam is focused into an image on the sample and is smaller than the sample so that no radiation reaches the sample edge. The advantage of using a focused spot smaller than the sample is that all of the radiation falling on the sample and reflected from it may be used in the reflectance measurement and calculation.

The lamp filament and the source optics are so oriented that a slightly defocused, narrow ribbon of light is imaged centrally on the circular sample surface when the incident angle is normal.

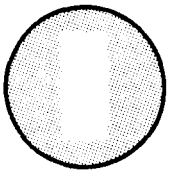

$\psi = 0$
Normal

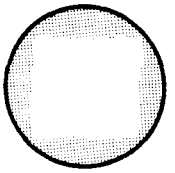

$\psi = 72^{\circ}$
Glancing

This ribbon image spreads to an approximately square image of suitable size on the sample when the incident angle becomes glancing (see accompanying sketch). The intensity of the image on the sample need not be evenly distributed or even have any prescribed intensity distribution over the face of the sample.

The collector of radiation is a large housing containing a well-defined square aperture, a front-surfaced paraboloidal mirror, a flat mirror, two double-ground quartz (or glass) diffusing screens, any one of four interference filters, and any one of three photomultipliers. The UV (0.2μ) interference filter was purchased at Thin Film Products, Cambridge, Massachusetts; the blue (0.4μ), red (0.65μ), and IR (1.0μ) filters were purchased from Optics Technology, Palo Alto, California. The photomultipliers are RCA Type 7200 for UV, Type 1P28 for blue and red, and Type 7102 for IR.

The source and collector optics are coated with magnesium fluoride for UV to IR reflectance.

The collection beam has the shape of a square cone of size

$$\Delta\phi = 18.47^{\circ}$$

$$\Delta\theta = 18.47^{\circ}$$

D. MEASUREMENT ANGLES

This apparatus permits use of the contiguous-panel method for sampling virtually all the radiation leaving the specimen. The hemisphere surrounding the sample is divided into contiguous square panels, each equal to the size of the collector optics ($18.47^{\circ} \times 18.47^{\circ}$). Each panel represents successive locations of the collector; the arrangement is analogous to covering an igloo with square shingles, each just touching the next, so that the total area of the shingles equals the total surface area of the igloo.

The measurement procedure is to lock the incident beam at a chosen incident angle (ψ_I, 0) and then to move the collector beam

successively through a set of positions (ϕ_J, θ_K). The reading obtained at each position contributes to the value of an over-all integral.

With this arrangement, the total radiation leaving the sample through the hemisphere is determined directly as the sum of all the readings at all the panel positions. The reflectance is calculated by dividing the sum of the panel readings by the reading for the incident beam.

The shape of the collector optics (and thus the shape of the panels) is square. Near the polar regions of the hemisphere, the arrangement of the squares necessarily becomes disordered. Their edges overlap at some points and fail to meet at others. The fact that some small areas are not covered while others are covered twice does not introduce error, so long as gaps and double coverages are, on the average, equal and evenly distributed; that is, the zone area and the total of the panel areas representing it must be precisely equal.

Each reading should be taken at a particular angular point on the hemisphere.

A satisfactory procedure is to divide the hemisphere that surrounds the sample into zones of 20^o width. The first zone is the polar cap defined by $\phi = 10^o$. The next zone extends from $\phi = 10^o$ to 30^o, the third $\phi = 30^o$ to 50^o, the fourth $\phi = 50^o$ to 70^o, and the fifth, the zone around the horizon, $\phi = 70^o$ to 90^o. The center of each zone and each panel in that zone lie at five mid-angles for the five zones. The first zone is a special case; its center is at $\phi = 0^o$, the pole. The centers of the other zones are at 20^o, 40^o, 60^o, and 80^o.

Each zone is filled with as many panels as precisely fill, and equal, the area of the zone. The number of panels in each zone and the center spacing between each panel in the zone is calculated by equating the product of the collector solid angle and the number of panels with a second quantity, the solid angle subtended by the zone, 2π ($\cos \phi_t - \cos \phi_b$), where ϕ_t is the angle of the top bound of the zone and ϕ_b is the angle of the bottom bound of the zone.

The necessary number of readings is reduced by a factor of two by reading over half a hemisphere and doubling the sum of the readings. The assumption is made that the sample is symmetrical about the plane of incidence--i.e., that the shape of the photometric lobe is the same on one side of the plane of incidence as on the other. This is a good assumption for almost all materials.

On the basis of the foregoing, readings are taken at 31 points on a half-hemisphere, as shown in the attached table. The number of panels in each zone is indicated as well as the angular increment between panel centers in each zone. The readings for all panels are summed directly, except that the reading from the last panel (negative angle) in each zone, which only partly laps into the half-hemisphere being measured, is multiplied

by a fractional constant representing the portion of the panel that is used. For example, the reading at $\phi = 40^{o}$, $\theta = -13^{o}$ is multiplied by 0.059 before being added to the other six readings in the 40^{o} zone.

At some of the panel positions, the radiation source interferes mechanically with the collector optics and a reading cannot be taken. For these panel setting points the reading is approximated by parabolic extrapolation from two nearby panel readings.

TABLE B1

COLLECTION ANGLES FOR CONTIGUOUS PANELS

Zone Number	Zone Center, ϕ	Number of Panels in Zone from $\theta = 0$ to $\theta = 180°$	Angular Interval, $\Delta\theta$, Between Panel Centers	Collection Angle, θ									
1	0° (Polarcap)	0.412	--										180°
2	20°	3.224	55.836°	-15½°			40½°		96°			152°	
3	40°	6.059	29.709°	-13°	16½°		46½°	76°		105½°	135½°		165°
4	60°	8.163	22.051°	- 7½°	14½°	36½°	58½°		81°	103°	125°	147°	169°
5	80°	9.282	19.391°	- 4°	15°	34½°	54°	73½°	92½°	112°	131½°	151°	170½°

APPENDIX C

ATMOSPHERE BAG

A relatively pure argon atmosphere can be obtained around a sample in four possible ways: a large, rigid-walled (evacuatable) chamber around the entire apparatus; a nonevacuatable bag or shell around the entire apparatus which is maintained at one atmosphere and in which the atmosphere is gradually purified by flow of clean argon through the shell; a small hemispherical quartz dome around the sample and rf concentrator; or a collapsible bag around the entire apparatus. The large evacuatable chamber is the most efficient in gas conservation but is economically out of the question. The shell which is purified by gas flow is more wasteful of argon than the other methods and slower. The use of a quartz dome necessitates reflectance measurements by transmission through the dome, a potential source of error. The collapsible bag is practical for our purposes.

A plastic bag about three feet in diameter, inflated, surrounds the entire apparatus. It is successively collapsed onto the apparatus (evacuated with a vacuum cleaner) and reinflated with pure argon several times until the desired purity of atmosphere is achieved.

The final purity can be calculated. In any such apparatus there will be a minimum of residual noncollapsible air pockets in the apparatus. The concentration of air remaining after several collapses is

$$C_n = (C_1)^n$$

where

C_n is the concentration of air in the final atmosphere.

C_1 is the concentration of air in the argon after the first collapse, which is also a measure of the fractional residual air pockets.

n is the number of collapses.

Typical values are C_1 = 5% residual air pockets and n = 4 successive collapses. The final atmosphere after four successive collapses will contain $(.05)^4$ or approximately 1 part in 10^5 of air and the remainder argon.

This method and this estimate assumes good stirring in the bag. Stirring is induced by jetting the inflow of argon at the proper point and direction in the bag.

APPENDIX D

CALCULATION OF REFLECTANCE

A. DATA FORMAT

A standard data sheet format is used for all experiments, as shown in Figure D1.

Figure D2 shows the data from a typical experiment, Exp. No. 57B. The data sheet is laid out in a matrix, the vertical on the data sheet representing vertical angles on the coordinate hemisphere and the horizontal representing horizontal angles on the hemisphere.

The data sheet contains a box for each of the 31 standard collection angle positions (see Table B1). As the equipment is set at each angle a reading is taken and recorded in the corresponding box.

The symbols in the boxes have the following meaning:

V_S is signal voltage read on the output voltmeter

V_N is noise voltage read on the output voltmeter

D_S is a Helipot dial setting ranging from 90 to 1000

The measurement procedure at each angle is to set the Helipot so that V_S is some reasonable value (typically 0.750 volt) and then record the Helipot setting.

V_N is the noise signal alone when an automatic shutter obscures the radiation source from the sample. For cold reflectance, V_N is zero and is customarily not read. For hot samples, a typical value of V_N might be 0.250 volt. In any given box on the data sheet V_N is always read at the same Helipot setting as V_S.

The calculation procedure is to divide V_S by D_S to obtain the "y" value for the box. Where noise is present, V_N is used as described in Appendix E to obtain a corrected value of the signal, V_S', which is then divided by D_S.

V_S/D_S (or V_S'/D_S) has the units of current and is represented by a current equal to the number of electrons per second in the phototube output, which in turn is proportional to the number of photons per second that are reflected from the sample into the phototube. Thus when the currents in all the data boxes are summed, they represent a number proportional to the total number of reflected photons per second (in a chosen wavelength band) leaving the sample in all directions.

DATA SHEET

PAGE 1 OF 2

EXP #
PURPOSE:

DATE

SAMPLE TYPE:

CONDITIONS : λ=..... SAMPLE TEMP..... ATMOS.....

RESULTS/COMMENTS:

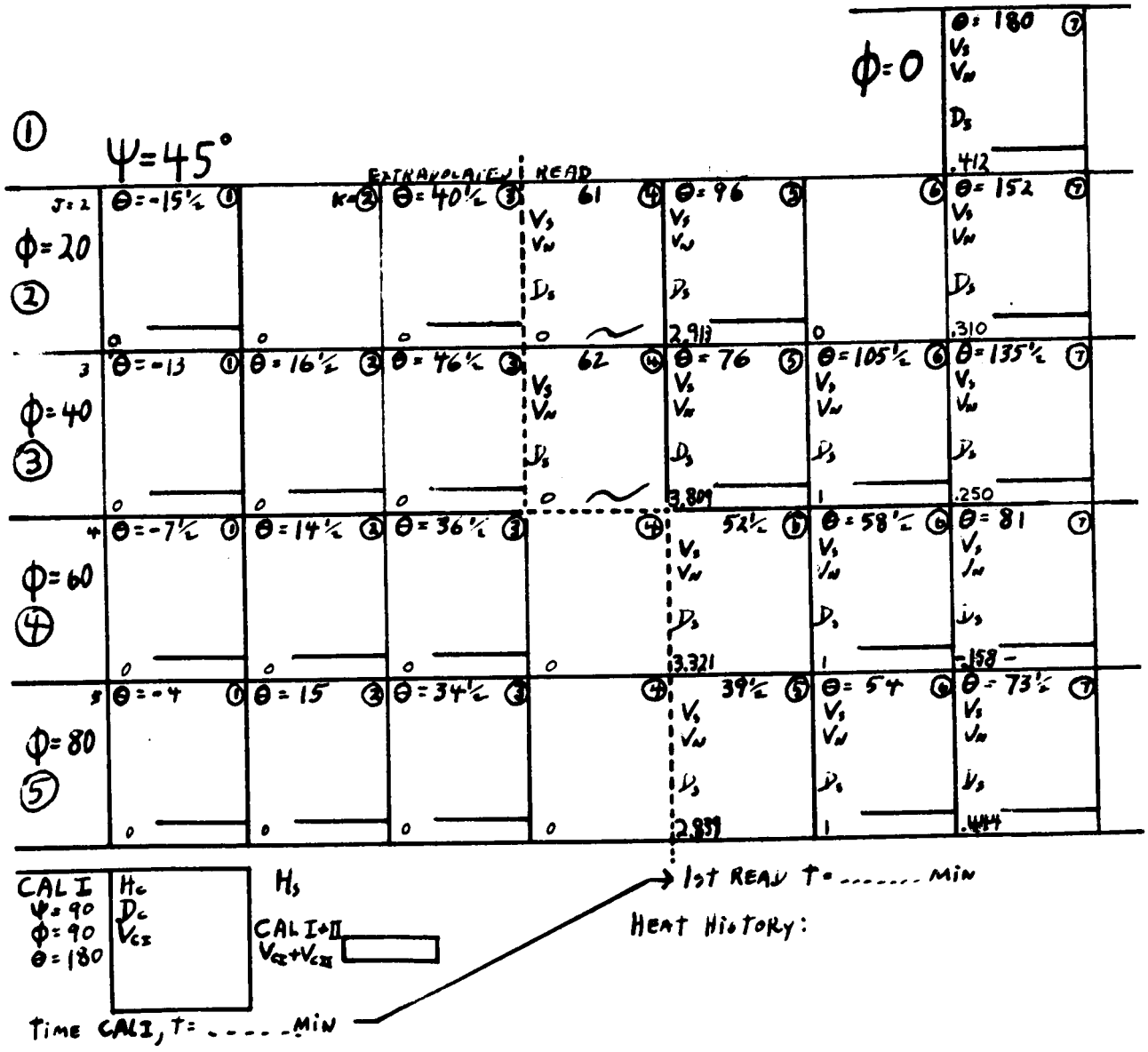

FIGURE D1 - FORM FOR RECORDING EXPERIMENTAL DATA (SHEET 1)

DATA

EXP #
SAMPLE DETAIL:

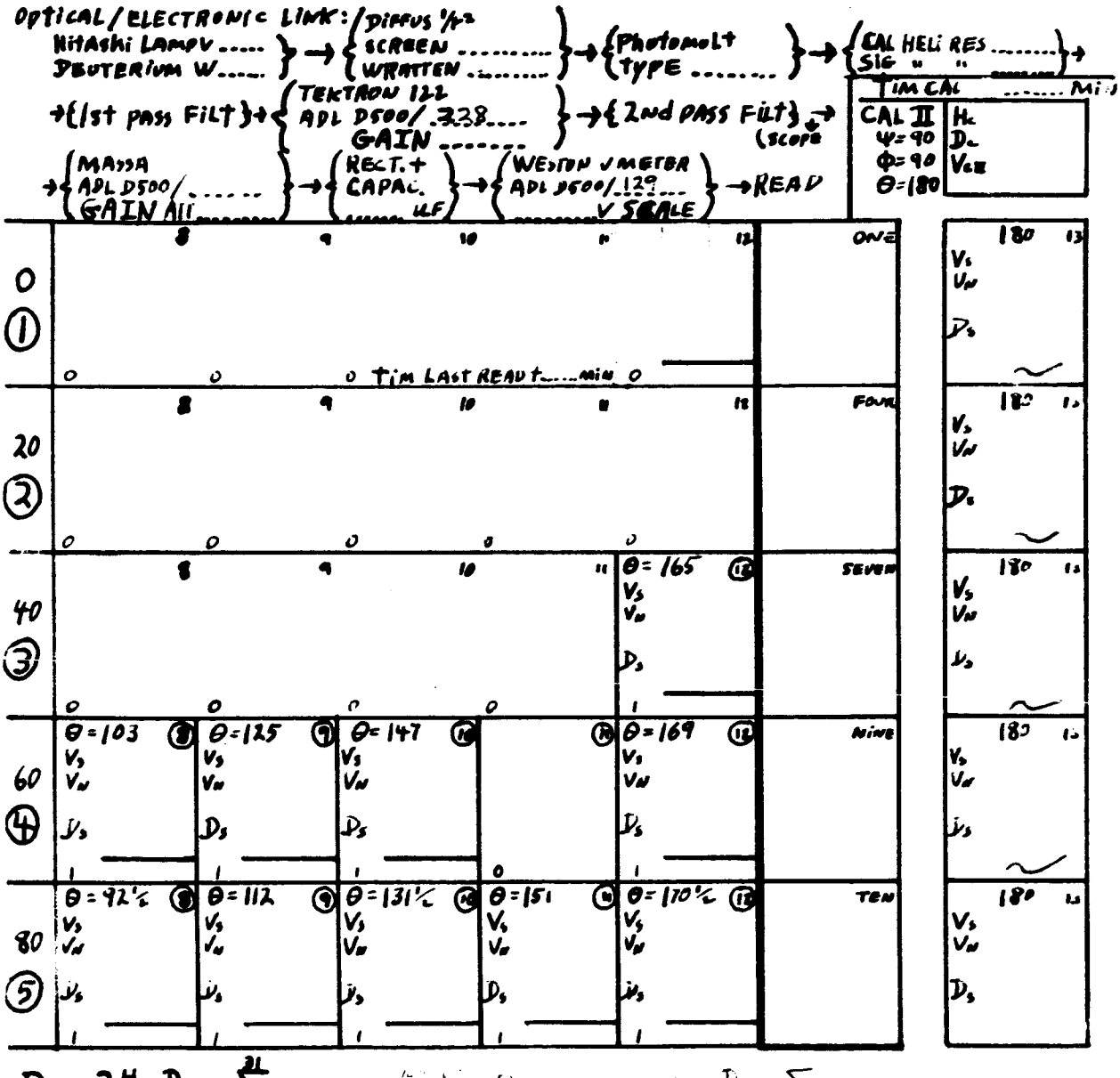

$$R_\psi = \frac{2H_c}{H_s}\frac{D_s}{V_c} A \sum_1^{21} y_{jk} \qquad R_\psi = 2.268\times10^{-3}\frac{D_s}{V_{cI}+V_{cII}}\sum y$$

V_s = SIG VOLT READ
V_N = NOISE " "
V_c = CAL " "
D_s = SIG HELIPOT DIAL READ
D_c = CAL " " "
A = (NEW) APERTURE FACTOR = 1.1143

R_ψ = {DIRECTIONAL SPECTRAL REFLECTANCE

H_s = SIG HELIPOT TOTAL RES. $49.12\times10^3\,\Omega$
H_c = CAL " " " $25.00\,\Omega$

y is READ FROM EACH BOX IN WHICH IT APPEARS (REFER CALC. PROCED.) } $\frac{V_s - V_N}{D_s} = y'$ or y is EXTRAP. DFC

FIGURE D1 - (Cont.) - FORM FOR RECORDING EXPERIMENTAL DATA (SHEET 2)

66558

DATA SHEET

EXP # 57B PAGE 1 OF 2 DATE 14

PURPOSE: Rerun earlier Exp (54A, B, C, D), 80-100 I mesh Clay

SAMPLE TYPE:

CONDITIONS: λ= blue SAMPLE TEMP cold ATMOS air

RESULTS/CONCLUS:

R = 7.882 %

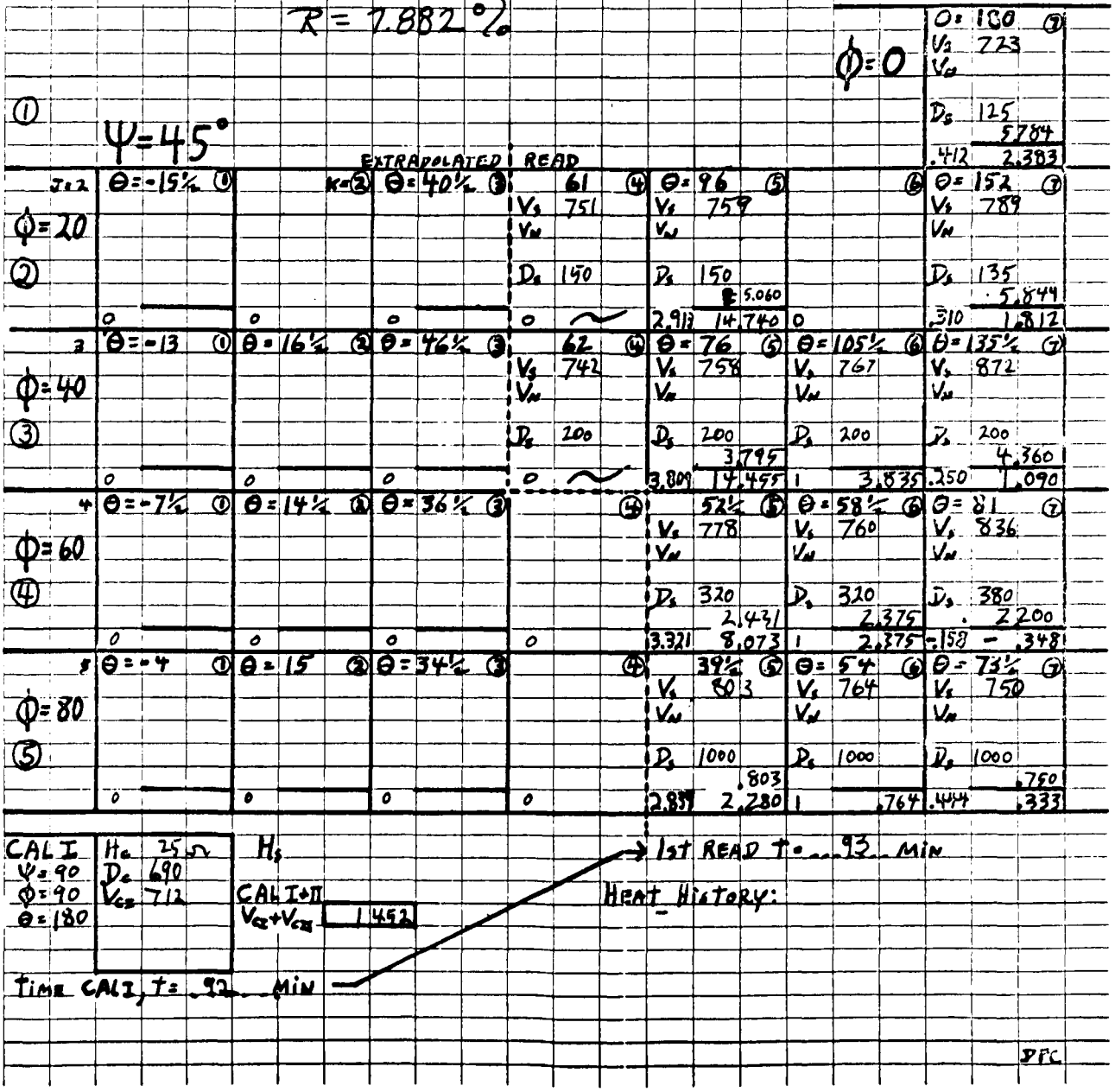

FIGURE D2 - TYPICAL DATA (SHEET 1)

DATA

66658

Exp # 578 PAGE 2 OF 2

SAMPLE DETAIL:

$\psi = 45°$

OPTICAL/ELECTRONIC LINK: Hitachi Lamp V ... 12 / Deuterium W ... → {Diffus 1/2 ✓ / Screen ... n.a. / Written ... 0} → {Photomult Type ... 1P28} → {CAL HELI RES ... / SIG " " ...} → TIM CAL .107 ... Min

→ {1st pass Filt} → {Tektron 122 / ADL D500/ .328 ... / GAIN ... 100} → {2nd pass Filt} → (scope)

→ {MASSA / ADL D500/ .12 ... / GAIN ATT 4.7dB} → {Rect.+ / Capac. / .80 uF} → {Weston Vmeter / ADL D500/ .129 ... / 1 ... V SCALE} → READ

CAL II	
ψ=90	H_c 25
Φ=90	D_c 690
θ=180	V_{cc} 740

	8	9	10	11	12	ONE	180 13
0							V_s / V_N
①							D_s
	0	0	0 tim LAST READ t 106 min		0	2,383	~
	8	9	10	11	12	FOUR	180 13
20							V_s / V_N
②							D_s
	0	0	0	0	0	16,552	~
	8	9	10	11	θ=165 ⑫	SEVEN	180 13
40					V_s 772		V_s / V_N
③					V_N / D_s 135		D_s
	0	0	0	0	1 5,718	25,098	~
	θ=103 ⑧	θ=125 ⑨	θ=147 ⑩	⑪	θ=169 ⑫	NINE	180 13
60	V_s 816 / V_N	V_s 870 / V_N	V_s 747 / V_N		V_s 764 / V_N		V_s / V_N
④	D_s 380	D_s 380	D_s 260		D_s 200		D_s
	1 2,147	1 2,289	1 2,873	0	1 3,820	21,229	~
	θ=92½ ⑧	θ=112 ⑨	θ=131½ ⑩	θ=151 ⑪	θ=170½ ⑫	TEN	180 13
80	V_s 727 / V_N	V_s 682 / V_N	V_s 724 / V_N	V_s 745 / V_N	V_s 770 / V_N		V_s / V_N
⑤	D_s 1000	D_s 1000	D_s 1000	D_s 750	D_s 565		D_s
	1 .727	1 .682	1 .724	1 .993	1 1.362	7,856	

$$R_\psi = \frac{2 H_c}{H_s} \frac{D_c}{V_c} A \sum_1^{21} y_{jk}$$, FOR {44 MK / 25 MN} $R_\psi = 2.268 \times 10^{-3} \frac{D_c}{V_{cc} + V_{cc}} \sum y$ 73.118

V_s = SIG VOLT READ

V_N = Noise " "

V_c = CAL " "

D_s = Sig HELIPOT DIAL READ

D_c = CAL " " "

A = (NOW) APERTURE FACTOR = 1.1143

R_ψ = {DIRECTIONAL SPECTRAL REFLECTANCE} $= 2.2685 \times 10^{-3} \frac{690}{1466} 73.118$

$= \cancel{7.807\%}$ 7.882%

H_s = SIG HELIPOT TOTAL RES. 49.12 x 10^3 Ω

H_c = CAL " " " 25.00 Ω

($\log_{10}$ 2.268.. = .35574)

y is READ FROM BACK BOX IN WHICH IF ANSWERS (REFER CALC PROCED.) $\frac{V_s - V_N}{D_s} = y'$ or y is EXTRAP. DFC

FIGURE D2 (Cont.) - TYPICAL DATA (SHEET 2)

B. EXTRAPOLATION

For some angles it is not possible to take readings because of mechanical interference between source and collector optics. At these angles a reading is estimated by extrapolation on the basis of nearby readings. For example, the data in the two boxes ($\phi = 40^{\circ}$, $\theta = 76^{\circ}$) and ($\phi = 40^{\circ}$, $\theta = 135\frac{1}{2}^{\circ}$) are used to predict data for the boxes ($\phi = 40^{\circ}$, $\theta = -13^{\circ}$) ($\phi = 40^{\circ}$, $\theta = 16\frac{1}{2}^{\circ}$), and ($\phi = 40^{\circ}$, $\theta = 46\frac{1}{2}^{\circ}$).

In some cases the apparatus can be set at more favorable angles for extrapolation than the nearest standard angle. In this case, a non-standard reading is taken at this more favorable angle and used for extrapolation only.

A parabolic extrapolation law was chosen because it is simple, smooth, and has zero slope at $\theta = 0$.

$$y = \alpha\theta^2 + \beta \tag{D1}$$

where

y is a reading

θ is the horizontal angle

α, β are coefficients

All the materials measured may be assumed to have a photometric lobe that is symmetrical about the plane of incidence. For a photometric lobe to be continuous at the plane of incidence, i.e. at $\theta = 0$, and also to be symmetrical,

$$\frac{dy}{d\theta} = 0 \quad \text{at } \theta = 0 \tag{D2}$$

Given two readings (for example $y_{3,5}$ at angle θ_5 and $y_{3,7}$ at angle θ_7) it is desired to predict a third $y_{3,K}$ at angle $\theta_{3,K}$.

If Eqs. (D1) and (D2) are combined, the resulting extrapolation formula is

$$y_{3,K} = \left[\frac{\theta_{3,7}^2 - \theta_{3,K}^2}{\theta_{3,7}^2 - \theta_{3,5}^2}\right] y_{3,5} - \left[\frac{\theta_{3,5}^2 - \theta_{3,K}^2}{\theta_{3,7}^2 - \theta_{3,5}^2}\right] y_{3,7} \tag{D3}$$

A considerable simplification in computation results by using chosen fixed angles (data boxes) on which to base all extrapolations such as θ_5 and θ_7. Thus Eq. (D3) reduces to an equation of the form

$$y_{3,K} = Ey_{3,5} - Fy_{3,7} \tag{D4}$$

where

E and F are numerical constants different for each box which is to be extrapolated.

It turns out to be unnecessary to predict a value for each unknown box on the data sheet. If each box were predicted, its value from Eq. (D4) would be added to the values of its neighbors to arrive at a summation for the 31 boxes. Thus the individual prediction can be bypassed and carried out in one step by an equation of the form

$$\sum_{K=1}^{n} y_{3,K} = \sum_{K=1}^{n} \left[Ey_{3,5} - Fy_{3,7} \right] \tag{D5}$$

where

n is the number of boxes in the zone (e.g., Zone 3) that need to be extrapolated.

Equation (D5) can be rewritten

$$\sum_{K=1}^{n} y_{3,K} = \left[\sum_{K=1}^{n} E \right] y_{3,5} - \left[\sum_{K=1}^{n} F \right] y_{3,7} \tag{D6}$$

or

$$\sum_{K=1}^{n} y_{3,K} = C' y_{3,5} - C'' y_{3,7} \tag{D7}$$

This means that there are two numerical coefficients, C' and C'', which, if multiplied by $y_{3,5}$ and $y_{3,7}$ respectively, will accomplish the necessary extrapolation for that zone. If the extrapolation value $y_{J,K}$ is at a standard angle θ_K, the value $y_{J,K}$ must be multiplied by $(1 + C')$ to account for its regular reading function as well as its extrapolation function. If y is at a non-standard angle, the value y is multiplied by C' (that is, $0 + C'$) as in Eq. (D7).

In Figure D1, each box upon which extrapolation is based contains a coefficient. For example at $\phi = 40^{\circ}$ and $\theta = 76^{\circ}$, the coefficient is 3.809. The value of this coefficient has been obtained by the method of Eq. (D7). The coefficient is multiplied by the calculated current V_S/D_S for the box, and the value is contributed to the reflectance integral.

For the sake of uniformity and accuracy all data boxes on the data sheet contain a coefficient written in the lower left hand corner. This coefficient has some positive or negative value (such as +3.809) where extrapolation is involved, 1.00 where the value for the box is to be used as is, and zero where the purpose is to assure that the box not be used.

C. CALCULATION OF REFLECTANCE

Reflectance, the ratio of reflected to incident radiation, is obtained from this apparatus in the following form:

$$R_{\psi\lambda} = \frac{2 \sum_{1}^{31} \frac{V_S}{(D_S/1000)H_S}}{\frac{V_C}{(D_S/1000)H_D}} \qquad \text{(D8)}$$

where the numerator is the sum of the photomultiplier output currents representing all the panel readings of reflected radiation, and the denominator is the photomultiplier output current representing the incident reading. The factor of two corrects for the fact that only half of the hemisphere is read. No detector aperture size enters Eq. (D8), because the total area of successive detector positions equals the area of the hemisphere.

Equation (D8) has been modified in three ways. The table of angles in Appendix B was calculated early in the program on the basis of a collecting aperture of $19^\circ \times 20^\circ$ (the paraboloidal mirror aperture). Later a more precisely defined aperture plate preceding the mirror was felt necessary; its size was $18.47^\circ \times 18.47^\circ$. Instead of recalculating the collection angles, it was simpler and sufficiently accurate to multiply Eq. (D8) by an aperture factor, A, equal to the ratio of the solid angles subtended by the old and new apertures:

$$A = \frac{(19^\circ \times 20^\circ)}{(18.47^\circ \times 18.47^\circ)} = 1.1143$$

Two other changes in Eq. (D8) are made for convenience. A pair of incident readings are taken, one before and one after the reflected summation, and the average incident reading is used in the denominator of Eq. (D8). The factor of two in averaging may be put into Eq. (D8).

The remaining modification to Eq. (D8) consists of entering the signal Helipot resistance value ($H_S = 49.12 \times 10^3$ ohms) and the incident Helipot resistance value ($H_D = 25.00$ ohms) used throughout the program. These values, combined with the factor of 2 needed to average the pair of incident readings, cause Eq. (D8) to assume the following form:

$$R_{\psi\lambda} = 2.268 \times 10^{-3} \frac{D_C}{V_{CI} + V_{CII}} \sum_{1}^{31} (\text{coeff}) \frac{V_S}{D_S} \qquad \text{(D9)}$$

D. CALCULATION BY HAND

For manual calculation of the reflectance, each block of the data sheet is treated as follows: V_S is divided by D_S, and the quotient is multiplied by the coefficient written in the lower left hand corner of the block. The resulting product is called y. The y's for all blocks are summed and multiplied by the term before the summation, as shown in Eq. (D9), resulting in a value of reflectance $R_{\psi\lambda}$. On many desk calculators the y summation can be automatically accumulated, which saves time and reduces chance of error.

E. CALCULATION BY COMPUTER

A computer program was written to calculate Eq. (D9) from the data sheets. It proved more efficient to store the block coefficients in the computer memory than to enter them for each reflectance calculation. Each block of the coordinate hemisphere and data sheet was given a two-dimensional subscript (J,K), where J and K identify the row and column of the matrix respectively.

As is apparent from Figures D1 and D2, J has integral values 1 through 5 and K has integral values 1 through 12. The coefficient associated with each block is stored by subscript J, K in the computer.

A signal current is calculated for each block and multiplied by its corresponding coefficient; the currents are then summed and multiplied by the terms to the left of the summation in Eq. (D9).

The program was written for use on an electronic computer via a teletypewriter. The computer is situated at Bolt Beranek and Newman, Inc., of Cambridge, Massachusetts.

Definitions of terms, a flow chart, and program listing are shown in Table D1, Figure D3, and Figure D4 respectively.

TABLE D1

COMPUTER PROGRAM NOMENCLATURE

Laboratory Data Sheets	Computer Program	Designates
A	A	Aperture factor
Ψ	ANG	Angle of inclination
	CC [J,K]	Coefficient for a block in matrix
D_C	DC	Incident Helipot dial setting
D_S	DS [J,K]	Signal Helipot dial setting
H_C	HC	Incident Helipot total resistance
H_S	HS	Signal Helipot total resistance
	J	Subscript for row of matrix (i.e., zone)
	K	Subscript for column of matrix
	L	Index for program logic
	M	Index for program logic
	N	Index for program logic
ϕ	PHI [J]	Zone of sphere
R_Ψ	R	Reflectance of sample
Σy_{JK}	S	Sum of signal currents
θ	T [J,K]	Angle of reflection
$V_{CI} + V_{CII}$	VCS	Sum of incident voltage reading
V_N	VN [J,K]	Noise voltage reading
V_S	VS [J,K]	Signal voltage reading
	Y [J,K]	Signal current

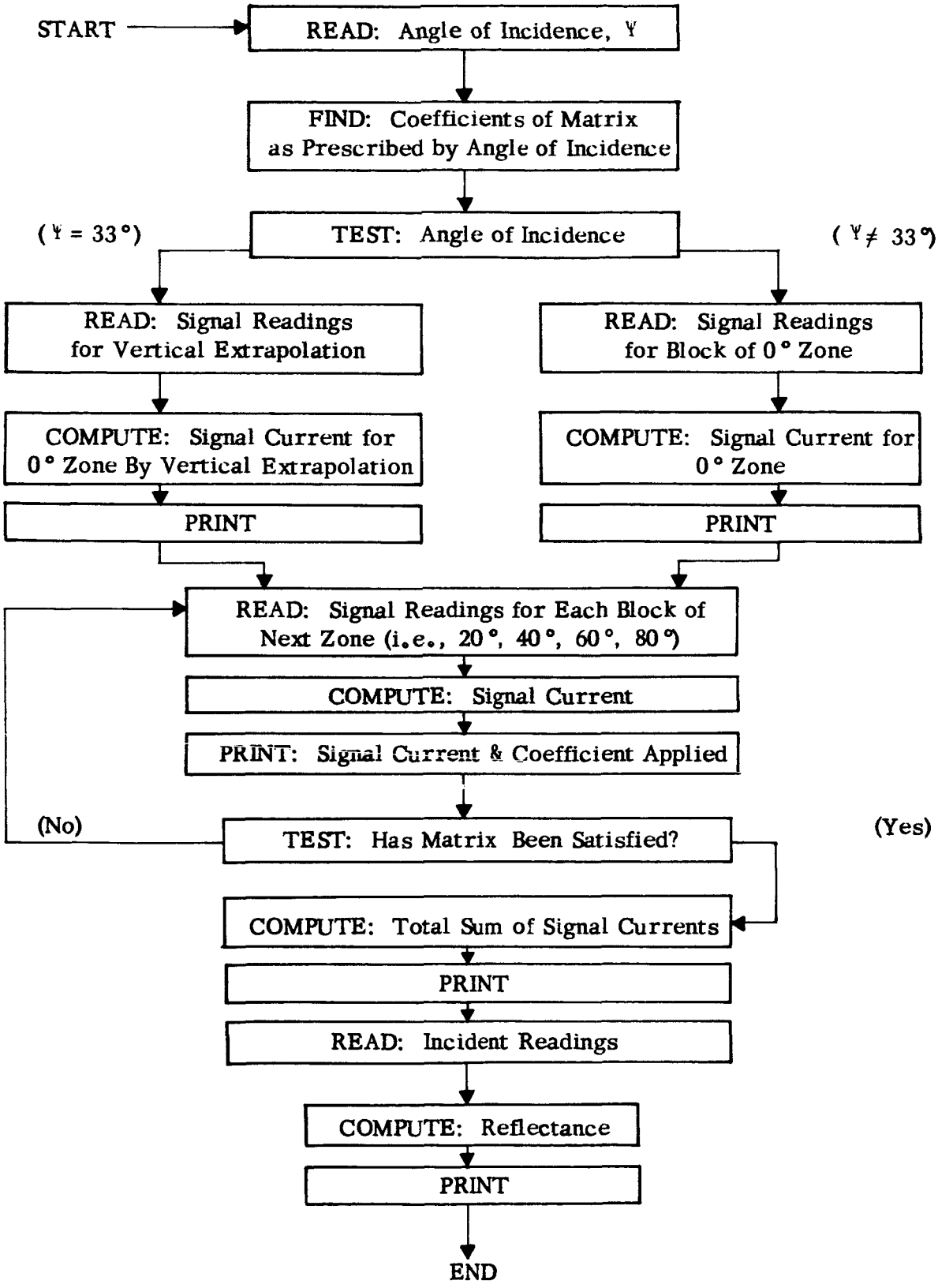

FIGURE D3 - FLOW CHART FOR COMPUTER CALCULATION OF REFLECTANCE BY CONTIGUOUS PANEL METHOD

```
2.00;COEFFICIENTS FOR BLOCKS
2.001 DEMAND ANG
2.0011 CC[N,13]=0 FOR N=1:1:5
2.0012 CC[2,13]=.549332 IF ANG=33
2.0013 CC[3,13]=-.137332 IF ANG=33
2.01 CC[1,12]=.412256,CC[2,5]=2.9138
2.02 CC[2,6]=0,CC[2,7]=.30992
2.03 CC[2,N]=0 FOR N=8:1:12
2.04 CC[3,5]=3.8094
2.05 CC[3,5]=4.3722 IF ANG=33
2.06 CC[3,6]=1,CC[3,7]=.2493
2.07 CC[3,7]=-.31349 IF ANG=33
2.08 CC[3,N]=0 FOR N=8:1:11
2.09 CC[3,12]=1,CC[4,5]=3.32199
2.10 CC[4,6]=1,CC[4,7]=-.15909
2.11 CC[4,N]=1 FOR N=8:1:10
2.12 CC[4,11]=0,CC[4,12]=1,CC[4,13]=0
2.13 CC[5,5]=2.83969,CC[5,6]=1,CC[5,7]=.442704
2.14 CC[5,N]=1 FOR N=8:1:12
2.15 CC[5,13]=0
2.16 TO PART 3

3.00;REFLECTANCE CALCULATION,VERTICAL EXTRAPOLATION
3.012 TYPE FORM 1
3.02 LINE
3.04 PHI[1]=0
3.05 TO STEP 3.20 IF ANG<>33
3.06 DEMAND VS[J,13],VN[J,13],DS[J,13] FOR J=2:1:3
3.061 Y[J,13]=(VS[J,13]-VN[J,13])/DS[J,13] FOR J=2:1:3
3.07 Y[1,12]=Y[2,13]*54.9332*10↑(-2)-Y[3,13]*13.7332*10↑(-2)
3.08 TYPE PHI[1],Y[1,12]
3.09 LINE
3.10 M=2,L=5,S=Y[1,12],PHI[2]=20
3.101 TYPE PHI[2]
3.11 TO STEP 3.23
3.20 M=1,L=12,S=0,Y[1,5]=1,Y[1,7]=1
3.21 TYPE PHI[1]
3.23 DO PART 4 FOR K=L:1:13 FOR J=M:1:5
3.24 TO PART 5

4.00 ;REFLECTANCE CALCULATION
4.01 Y[J,K]=0 IF CC[J,K]=0
4.02 TO STEP 4.26 IF CC[J,K]=0
4.101 CC[3,13]=-.137332 IF ANG=33
4.23 DEMAND VS[J,K],VN[J,K],DS[J,K]
4.24 Y[J,K]=(VS[J,K]-VN[J,K])/DS[J,K]
4.25 S=S+CC[J,K]*Y[J,K]
4.26 TYPE Y[J,K],CC[J,K]
4.261 LINE
4.262 TO STEP 4.27 IF K<13
4.263 PHI[J+1]=PHI[J]+20
4.2631 LINE
4.2632 TYPE PHI[J+1]
4.27 L=5

5.00 LINE
5.001 TYPE S
5.002 DEMAND DC,VCS
5.0021 A=1.1143,HS=49.12*10↑3,HC=25.0
5.02 R=4*HC*A*DC*S/(HS*VCS)
5.03 TYPE FORM 1,R*(10↑2)
5.04LINE
5.05 TYPE"TO START NEXT RUN RETYPE FORM 1,...DO PART 2"
```

FIGURE D4 - PROGRAM LISTING

APPENDIX E

DISCUSSION OF ERRORS

Sources of error in these measurements may be classed as errors of apparatus and errors of results. Two guides for statistical treatment of the data have been Cameron's chapter on statistics and discussion on the design of experiments* and Hoel on estimates with small samples**.

A. SUMMARY OF ERRORS

Following Cameron*, an estimate of accuracy can be based on a multiple (such as 2) of the standard deviation calculated from the measured data plus an estimate of other errors known to exist in the system. Table E1 shows an over-all accuracy based on estimates developed in later sections of this Appendix.

TABLE E1

CALCULATION OF OVER-ALL ACCURACY

Type of Error	Cold Reflectance	Hot Reflectance
2 (σ = 5.2%)	± 10.4%	± 10.4%
Extrapolation	± 2.5%	± 2.5%
Quartz Diffuser	± 2.8%	± 2.8%
Electronic Drift	± 0.5%	± 0.5%
Random Noise at 2200°F	--	± 2.0%
Noise Drop-off Effect	--	± 2.0%
	± 16.2%	± 20.2%

To summarize, the over-all accuracy is estimated to be within ± 16% for cold reflectance or ± 20% for hot reflectance, and the precision for each is σ = 5%.

---

* Joseph M. Cameron, "Design of Experiments", Sect. 12 in Vol. I, Chap. 2 of Fundamental Formulas of Physics, D. Menzel, ed., New York, Dover, 1960.

** Paul G. Hoel, Introduction to Mathematical Statistics, 2nd ed., New York, Wiley, 1955, pp. 196-200.

B. ERRORS OF APPARATUS

Sources of error in this apparatus may be classed as mechanical, optical, and electronic. In general, any influence causing a constant arbitrary change in gain or response of the system is of no consequence, because it affects incident and reflected readings alike, and only their ratio is used. If the arbitrary gain change influences incident and reflected readings unequally, an error is caused. The influence may operate unequally on incident and reflected readings either directly or through a time variation, since the two measurements are made at different times. Further, this influence may be biased, leading to systematic errors, or random, leading to random errors. All known systematic corrections were applied, to the point that residual errors were believed to be random and without bias.

1. Mechanical Errors

All aspects of the apparatus--its design, construction, initial alignment, and set-up procedure--contributed to high accuracy. Every part of the experiment, including the sample position, was within 20 mils of its correct position (and often 5 mils) in a coordinate hemisphere with an operating radius of 10 inches.

During an experiment, angles of incidence (ψ) and angles of collection (ϕ,θ) were determined by pointers and angle scales on the apparatus and were set by hand, always within ½ degree (often 0.1 degree). Angle setting also produced negligible error relative to other errors in the system.

A noticeable source of error is the interference between source and collector at certain angles. At these angles (region of backward scattering) readings cannot be taken, and values are extrapolated from nearby readings. Twenty-two collector positions (panel positions) are read; the other eleven must be estimated by extrapolation. The magnitude of the extrapolation error depends on the shape of the photometric lobe of the sample and on the angle of incidence. Consider a sample under normal incidence and of circular symmetry, so that the photometric lobe is cylindrically symmetric about the normal to the center of the sample. In this case, if one merely omitted the eleven extrapolated readings, the measured reflectance would be approximately (33-11)/(33) or 67% of its actual value. This statement includes the simplifying assumption that the omitted and included readings have the same average value. Now let us assume that the extrapolation is sufficiently correct to predict values within $\pm$ 20% of those that would be measured if they could be measured. In this case the true reflectance will be [67% + 33% $\pm$ (.2) 33%] = 100 $\pm$ 6.6% of its measured value.

The next refinement is to make some assumptions about the nature of any photometric lobe: 1) the sample is symmetric about the plane of incidence (thus the plane of incidence, which slices the photometric hemisphere into two equal halves, will slice the photometric lobe into

two halves, each the mirror image of the other, and any angle of incidence, not necessarily normal, may be assumed); and, 2) no abrupt discontinuity in the shape of the photometric lobe exists. Thus the slope of the photometric lobe near $\theta = 0$ must approach the same value from either half of the lobe--i.e., from either side of the plane of incidence.

There can be only one slope, zero, that meets these assumptions; stated mathematically, $\frac{dy}{d\theta} = 0$. A simple function that satisfies the assumptions and has zero slope at $\theta = 0$ is a parabolic law, which is the one used (see Appendix D).

The error in parabolic extrapolation depends on the nature of the sample. Parabolic extrapolation is completely correct for a Lambert's (diffuse) reflector, in which $\frac{dy}{d\theta} = 0$ at all points on the photometric lobe. We find that MgO is very close to a Lambert's surface. The chars also are quite similar to a Lambert's surface, as far as backward extrapolation is concerned, because they act like a diffuse material having an additional specular component as well as a very slight back-scattering component. The forward specular lobe is out of the region on which back extrapolation is based and, therefore, does not influence the extrapolation. The remaining component of reflection is substantially diffuse, for which the extrapolation is correct.

An estimate of the extrapolation errors of these tests would be: chars at near normal incidence ($\psi = 33^\circ$) and MgO approximately $\pm$ 0%; for chars at other incident angles ($\psi = 45^\circ, 60^\circ, 72^\circ$) and for pyrolytic graphite at all incident angles ($\psi = 33^\circ, 45^\circ, 60^\circ, 72^\circ$), error is in the range of $\pm$ 2.5% and random in the sense that no bias can be ascribed on the basis of previous knowledge.

2. Optical Errors

The size of the collecting aperture (that is, the panel size) and the ability of the front-surfaced mirrors to collect and transmit radiation to the photocell are well known and uniform to the extent that they give rise to negligible errors. The collector cone of $18.47^\circ \times 18.47^\circ$ collects all of the incident cone of $9.5^\circ \times 9.9^\circ$ with no loss.

The one substantial optical error in the system is due to a poorly functioning diffusing screen. Radiation passes through the collector aperture and onto a front-surfaced ellipsoid, which focuses an approximately one-to-one size image of the sample onto a diffusing screen. The purpose of the diffusing screen is to thoroughly mix radiation, both with respect to the angle of arrival through the collector aperture and with respect to the shape of the sample image. The intent is that a photomultiplier three inches behind the diffuser screen gives a reading proportional to the flux at the diffuser screen and independent of angle and position. In the visible blue and red, opal glass and/or a combination of three layers of ground glass and white bond paper prove to be excellent

diffusers. The output signal shows no change as a narrow beam is scanned across the collecting aperture.

When UV runs were begun, quartz diffusers were installed for all readings--UV, blue, red, and IR--in the interests of uniformity. Much of the early data on blue and red was taken with a glass and paper diffuser, but all the later readings were obtained with a quartz diffuser.

The quartz was a poor diffuser, no matter how its surface was ground or sandblasted and despite the fact that four sandblasted surfaces were used (two spaced sheets ground on both sides).

Following experiments with various quartz ground surfaces and geometries, it was decided to accept the poor diffusing qualities, to characterize the diffuser by measurements, and to take the character of the diffuser into account in determining reflectances.

The characteristic of the quartz diffuser, as with any poor diffuser, is that it passes a substantial forward lobe similar to ordinary transmission but considerably broadened. The effect in the apparatus is to make the sensitivity across the collecting aperture higher in the central regions and lower toward the edges. This non-flat response favors a narrow beam such as the 9.5 x 9.9 incident beam over a more broadly collected beam such as the sample reflected radiation (18.47^{o} x 18.47^{o}).

With quartz diffusers in place, the response across the collection aperture was carefully measured using a narrow test beam (1.3^{o} for the visible 2.2^{o} for the UV) for UV, blue, and red. IR was not tested. The collector aperture was broken into ten zones, and the area of each zone was multiplied by the sensitivity representation of that zone. The products were numerically integrated to give an over-all response for the aperture*. The process was then repeated for a smaller region in the middle of the aperture equal to the incident beam size. The ratio of the two summations, each normalized for its area, gave a factor, K, representing the performance of the diffuser. (K = 100% for a perfect diffuser and 80%-90% for a poor diffuser.) The K value was slightly different for each wavelength. At the UV, it was 87.0%; at the blue, 84.7%; at the red, 82.7%. The plot of the K value for UV, blue, and red was extrapolated to determine the IR value (81.5%).

Each reflectance taken from the data sheets for runs in which the quartz diffusers were used were divided by the appropriate K value to restore the reflectance to the value which would have been obtained with a perfect diffuser such as opal or paper.

---

* The integration was performed for a circle of equivalent area to the square aperture, a simpler and sufficiently accurate procedure.

The error introduced by the procedure of correcting for a poor diffuser may be estimated. The error in measured reflectance, if no diffuser correction is applied at all, is of the order of 20%. When the K correction is made, the error centers around zero, but a random error remains. This error depends on how accurately the quartz diffuser correction values were determined and applied. A reasonable estimate is that the drop from 1.00, i.e., (1 - K), was measured to within an accuracy of $\pm$ 15%. Then the resulting random error is (0.815 + 0.185 $\pm$ 15% of (0.185) = 1.00 $\pm$ 2.8%), or $\pm$ 2.8%.

3. Electronic Errors

Various tests were performed to determine how much error the electrical and electronic system could be expected to cause in the reflectance values. Sources of error are: gain drifts versus time, and non-linearity in this drift; gain changes versus signal level, i.e., non-linearity; and several random sources which can be classed as noise.

In the drift-versus-time tests, the first tests were to assess drifts in the source lamp and photomultipliers. All amplifiers were turned on and left on for three hours, so that steady gain could be assumed. Then, with the source beam aimed directly into the detector, the source lamp (with photomultiplier on) was turned on and off and the output was plotted versus time. The procedure was then repeated with the source lamp on and the photomultiplier turned on and off. When the lamp was turned on, there was a downward drift of signal of 3% per hour caused by lamp and amplifiers together. The photomultiplier exhibited negligible drift after turn-on (i.e., not different from 3%).

The drift of the whole system was tested in the same way. After a night's shut-down, all components--lamp, chopper, photomultiplier, and amplifiers, including output integration circuit and meter--were turned on at the same time (t = 0) in the morning, and the output signal was plotted against time.

The output showed an initial 4% drop during the first 15 minutes (16% per hour) and then settled out to a steady drift downward of 7.2% per hour for the first hour. Drift during the third hour was 3%, as mentioned above.

Since, in a reflectance run, the incident beam is read once before and once after the reflected readings and averaged, linear drifts in the apparatus cancel. The only significant cause of error is the non-linearity of drift with time. For the over-all time drift mentioned above, this non-linearity was found to be $\pm$ 0.42% $\approx \pm$ 0.5% maximum for the first hour and steadily less thereafter.

A subtler potential form of error is caused by drift of gain with time. A cold reflectance run takes one-half hour, a hot run about one hour; if the sequence of readings and the shape of the photometric lobe of the sample were such that all the important (high-intensity)

readings were taken early or late in the run, the measured reflectance would be correspondingly too high or too low by a small percentage. This potential error can be reduced to a negligible level by staggering the sequence of readings. The five zones are read starting at the bottom zone ($\phi = 90^{o} - 70^{o}$) and reading from $\theta = 0^{o}$ to $\theta = 180^{o}$. The next zone up ($\phi = 70^{o} - 50^{o}$) is read from $\theta = 180^{o}$ to $\theta = 0^{o}$, and so on.

Gain changes versus signal level for many types of signal measuring equipment can be considered to be a potential source of trouble, particularly in equipment such as this, in which the strongest radiation reading (incident) is some 2000 times as strong as the weakest reading (glancing collection at near-normal incidence). A Helipot normalizing scheme was used. A Helipot, operating directly on the output of the photomultiplier tube, was adjusted at each reading so that the signal voltage passing through the amplifiers and read on the output meter was approximately at a constant level for all incident and reflected readings. This level was chosen to be a suitable moderate and linear signal level for all the amplifiers and for the output meter. In practice, for a new sample of different reflectance than a previous sample (e.g., char followed by MgO), the amplifier gains were reset to again achieve the same moderate operating signal level. To span the range of 2000, two Helipots were used, one (25 ohms) suitable for the incident beam, and one (49.12K) suitable for the reflected readings. When two separate Helipots are used, the ratio of their individual resistances enters the equation for the calculation of reflectance. Their resistances were measured to better than $\pm$ 0.1% and are shown in Eq. (D9), Appendix D.

The burden of the constancy of gain versus signal strength in this apparatus falls on the detector. Most detectors are not capable of proper linear (or noise) operation over a dynamic range of 2000 to 1, but a photomultiplier is in fact linear over a far greater range. The only potential cause of non-linearity is dynode loading when dynode voltage dividing resistors are used. Loading causes dynode potential changes with signal level. By connecting tapped strings of batteries directly to the dynodes and by keeping the only resistor (the anode load resistor) low, 50K, a very linear photomultiplier response can be maintained. Each input photon generates approximately 10^{4} output electrons at the anode, virtually independently of how many photons are received. There is no lower limit to the linear range. The upper limit is characterized by current-saturation effects (electron multiplier ratio changes) at the anode and higher-current dynodes, a limit that was avoided. Errors due to change of gain with signal level are apparently negligible.

Several sources of random noise are identified in the following paragraphs; with one exception, an estimate of their effect is best obtained from the scatter in the measured reflectance points.

The most important random error occurs during hot sample measurements. The sample emits radiation; most of this is steady, but a small component is random. In turn, a component of this random signal is contained in the signal frequency band at 150 cps. As the sample

becomes hotter, more noise at 150 cps is emitted until the 150-cps reflected signal is exceeded and reflectance measurement becomes impossible. The maximum temperature at which it was found practical to make measurements on chars for all four wavelengths was 2200°F.

Randomness at 2200°F shows up as a randomness in output meter reading, despite the fact that the reading is already considerably smoothed by a 6-second integration circuit. The random variation in each meter reading is at most ± 10%. The approximate effective randomness of a composite reading made up of 22 independent, randomly varying readings is $\pm 10\%/\sqrt{22} = \pm 2\%$ with no appreciable systematic error in the meter reading process.

One mysterious electronic source of error associated with high-temperature measurements was characterized and removed from the calculations, but its cause is still unknown. The circuits normally perform the following functions: reject dc, selectively amplify 150-cps ac (the signal) detect (rectify) the signal, integrate the resulting dc, and indicate the dc signal on a dc voltmeter. The unexplained effect is this: as noise containing a component at the signal frequency is progressively introduced, either due to heating the sample or artificially, the reflectance signal is unexpectedly reduced. The more the noise, the lower the signal, until at a signal-plus-noise to noise ratio of 5.5 to 1 the signal plus noise drops to 81% of its noise-free value. The S + N value then stays at 81% until the noise has been increased to an S + N/N value of 2.5, at which point the S + N begins to increase with further addition of noise. The initial drop in S + N with increasing N is unexplained. The later increase of S + N with increasing N follows expected behavior.

Studies of this effect showed that it is quite reproducible. Tests were made with two adjacent samples, one hot and one cold. The beam was diverted to the cold sample to remove any question of sample change. The effect can be reproduced with a cold sample and artificial electrical noise injected at the photomultiplier load resistor. The rectifier, integrator, and meter circuit are not at fault. Output waveforms are as expected, and no noticeable biasing occurs. In several tests the circuits were deliberately worsened by degrees; one, for example, simulated an imperfect integrator. These tests all showed the expected effects and failed to shed any light on the cause of the effect being investigated. No studies have been made of effects inside the three commercial amplifiers used in the circuit.

Since the effect was quite reproducible, it was carefully characterized by feeding a fixed signal plus progressively increasing noise into the system, plotting the result, and drawing up a correction table. For all high-temperature readings, noise alone was read (incident beam off) and recorded as well as signal plus noise; both were read into the table, and a corrected "signal" value was read out.

The principle error caused by this correction procedure is due to whatever lack of precision may exist in the noise readings or in the noise correction table. The error in the application of the correction procedure appears to be random and to have a value of $\pm$ 2%.

The noise correction procedure has been checked in one IR reflectance run in which the 7102 photomultiplier was insufficiently cooled. Normally in high-temperature readings the incident reading contains negligible noise, while the reflected readings do contain noise, the level of which serves as the basis for correction of the reading. In this particular IR run, however, the noise was generated in the tube*; it therefore appeared in both the incident and reflected readings and could be expected ideally to have reduced both by the same factor. As usual in the high-temperature readings, signal-plus-noise (V_S) and noise-alone (V_N) readings were taken during the reflectance run. Reflectance then was calculated in two ways: 1) ignoring noise (on the basis of V_S only) and 2) using the noise correction procedure (with V_S corrected on the basis of V_N). The two methods showed good agreement (R_{33IR} = .07287 and .07224); the difference of less than 1% showed that the noise correction performed within this range of accuracy.

The randomness in reading the output meter for cold-sample reflectances was negligible. Likewise, the randomness in setting the Helipot potentiometer was negligible for both hot and cold runs. Each was typically less than ½% per reading; when the averaging effect of taking 22 readings was applied, errors were insignificant.

Two problems with components introduced random errors in the earlier data runs. Each was random, affecting both incident and reflected readings, and is best evaluated in terms of the scatter in the reflectance data itself. In the first case, photomultiplier battery fluctuations developed; these were traced to the unloaded batteries that fed only the lower current dynodes. Some 1.5-volt cells in each 45-volt pack developed reversed polarities and, in some cases, indeterminate and fluctuating polarities. A new set of batteries were installed, and a light resistive load for all batteries was placed in parallel with the photomultiplier. This action eliminated the problem.

The second problem was caused by a large-value, government-surplus capacitor which we used for signal integration. We thought this to be a bathtub type, but it was actually an unmarked electrolytic. The leakage had the effect of a resistive shunt to the output meter of unknown value, which in turn caused an unknown change in the gain of the system. Such a change is of no consequence if it stays constant, since it would affect incident and reflected readings by the same factor. Error arises, however, if this unknown resistance has a component that varies randomly with time; such a variation between incident and reflected readings

*Shot noise related to current flow. Dark-current noise was never approached in any of our experiments and was not a noise factor.

introduces a random variation in measured reflectance that is equally likely to be too high as too low. The error is best estimated in terms of scatter of measured reflectance values.

C. ERROR OF RESULTS

Many reflectance readings were taken at different angles, at different wavelengths, and on different materials; yet it was obvious that the same general level of variability appeared to characterize all of these readings.

A recognized procedure for estimating the variance (or standard deviation) among many small sets of data in which parameters vary slightly from one set to the next is to estimate a variance for each set with respect to the mean of the set, normalize each to a percentage variance, average these percentage variances, and finally take the square root of the average variance to obtain an estimate of the standard deviation of the population from which the sets were drawn.

The sets are very small, from 1 to 5 reflectance data points. References (2) and (3) point out that the usual standard deviation formula introduces a bias for small data sets and that to obtain an unbiased estimate of population variance the following form should be used (Reference 3, p. 198):

$$\sigma_{set}^2 = \frac{n}{n-1} S^2 \qquad \text{(E1)}$$

where

S^2 is the set variance.

n is the number of data points in the set.

σ^2 is the unbiased estimate of variance of the population, i.e., the variance that would be expected from a large set.

When the methods previously described are applied to the data measured in this program, the resulting over-all percentage standard deviation characteristic of the method is

$$\sigma = 5.2\%$$